AFRL-RB-WP-TR-2008-3107

Z-PIN STUBBLE TECHNOLOGY ADVANCED RESEARCH (ZSTAR)

Stephen B. Clay and Amanda K. Pommer

Advanced Structural Concepts Branch
Structures Division

APRIL 2008
Final Report

AIR FORCE RESEARCH LABORATORY
AIR VEHICLES DIRECTORATE
WRIGHT-PATTERSON AIR FORCE BASE, OH 45433-7542
AIR FORCE MATERIEL COMMAND
UNITED STATES AIR FORCE

NOTICE AND SIGNATURE PAGE

Using Government drawings, specifications, or other data included in this document for any purpose other than Government procurement does not in any way obligate the U.S. Government. The fact that the Government formulated or supplied the drawings, specifications, or other data does not license the holder or any other person or corporation; or convey any rights or permission to manufacture, use, or sell any patented invention that may relate to them.

This report was cleared for public release by the Air Force Research Laboratory Wright-Patterson Air Force Base (AFRL/WPAFB) Public Affairs Office and is available to the general public, including foreign nationals. Copies may be obtained from the Defense Technical Information Center (DTIC) (http://www.dtic.mil).

AFRL-RB-WP-TR-2008-3107 HAS BEEN REVIEWED AND IS APPROVED FOR PUBLICATION IN ACCORDANCE WITH ASSIGNED DISTRIBUTION STATEMENT.

*//Signature//

STEPHEN B. CLAY, Ph.D.
Project Engineer
Advanced Structural Concepts Branch
Structures Division

//Signature//

JOSEPH P. NALEPKA, Chief
Advanced Structural Concepts Branch
Structures Division

*//Signature//

DAVID M. PRATT, Ph.D.
Technical Advisor
Structures Division

This report is published in the interest of scientific and technical information exchange, and its publication does not constitute the Government's approval or disapproval of its ideas or findings.

*Disseminated copies will show "//signature//" stamped or typed above the signature blocks.

REPORT DOCUMENTATION PAGE

Form Approved
OMB No. 0704-0188

1. REPORT DATE *(DD-MM-YY)*	2. REPORT TYPE	3. DATES COVERED *(From - To)*
April 2008	Final	01 June 2003 – 28 February 2008

4. TITLE AND SUBTITLE
Z-PIN STUBBLE TECHNOLOGY ADVANCED RESEARCH (ZSTAR)

5a. CONTRACT NUMBER
In-house

5b. GRANT NUMBER

5c. PROGRAM ELEMENT NUMBER
62201F

6. AUTHOR(S)
Stephen B. Clay and Amanda K. Pommer

5d. PROJECT NUMBER
A03M

5e. TASK NUMBER

5f. WORK UNIT NUMBER
0B

7. PERFORMING ORGANIZATION NAME(S) AND ADDRESS(ES)
Advanced Structural Concepts Branch (AFRL/RBSA)
Structures Division
Air Force Research Laboratory, Air Vehicles Directorate
Wright-Patterson Air Force Base, OH 45433-7542
Air Force Materiel Command, United States Air Force

8. PERFORMING ORGANIZATION REPORT NUMBER
AFRL-RB-WP-TR-2008-3107

9. SPONSORING/MONITORING AGENCY NAME(S) AND ADDRESS(ES)
Air Force Research Laboratory
Air Vehicles Directorate
Wright-Patterson Air Force Base, OH 45433-7542
Air Force Materiel Command
United States Air Force

10. SPONSORING/MONITORING AGENCY ACRONYM(S)
AFRL/RBSA

11. SPONSORING/MONITORING AGENCY REPORT NUMBER(S)
AFRL-RB-WP-TR-2008-3107

12. DISTRIBUTION/AVAILABILITY STATEMENT
Approved for public release; distribution unlimited.

13. SUPPLEMENTARY NOTES
PAO Case Number: WPAFB 08-2565; Clearance Date: 07 Apr 2008. Report contains color.

14. ABSTRACT
Z-pins are small-diameter carbon rods that are ultrasonically inserted through composite laminates in the z-direction to provide extra resistance to crack growth and delamination. They are normally inserted through co-cured composites, but this report presents an experimental study on a new z-pin stubble manufacturing technique that is compatible with the co-bonding process. Early researchers were limited to an exposed stubble height of 0.030 inch, which would not provide all of the benefits of a full-depth co-cured z-pin reinforced joint. This report describes a study in which the stubble lengths were increased to 0.250 inch. Double cantilever beam specimens were used to characterize the effect of stubble diameter and height on the Mode I crack resistance. It was found that increasing the stubble height from 0.040 inch to 0.125 inch resulted in a significant improvement in Mode I properties.

Full Abstract on reverse side →

15. SUBJECT TERMS
z-pin, Z-Fiber™, stubble, ultrasonic insertion, composite, through-thickness reinforcement

16. SECURITY CLASSIFICATION OF:			17. LIMITATION OF ABSTRACT:	18. NUMBER OF PAGES	19a. NAME OF RESPONSIBLE PERSON (Monitor)
a. REPORT	b. ABSTRACT	c. THIS PAGE			Stephen B. Clay
Unclassified	Unclassified	Unclassified	SAR	62	19b. TELEPHONE NUMBER *(Include Area Code)* N/A

Standard Form 298 (Rev. 8-98)
Prescribed by ANSI Std. Z39-18

14. ABSTRACT (full)

Z-pins are small diameter carbon rods that are ultrasonically inserted through composite laminates in the z-direction to provide extra resistance to crack growth and delamination. They are normally inserted through co-cured composites, but this paper presents an experimental study on a new z-pin stubble manufacturing technique that is compatible with the co-bonding process. Z-pin stubble is created by inserting pins through the thickness of an uncured laminate and trimming the pins to a certain height above the surface. After initial cure, another uncured composite part is cured on the exposed stubble. Early researchers were limited to an exposed stubble height of 0.030 inch, which would not provide all of the benefits of a full-depth co-cured z-pin reinforced joint. This paper describes a study in which the stubble lengths were increased to 0.250 inch. Double cantilever beam (DCB) specimens were used to characterize the effect of stubble diameter and height on the Mode I crack resistance. It was determined that the new approach using a second ultrasonic step is indeed necessary for stubble heights on the order of 0.125 inch. It was also found that increasing the stubble height from 0.040 inch to 0.125 inch resulted in a much more significant improvement in Mode I properties than increasing the aerial density from 2% to 4%. Finally, taking that final step of increasing the stubble height from 0.125 to 0.250 inch did not improve the properties as much as would be expected from previous studies.

TABLE OF CONTENTS

LIST OF FIGURES

LIST OF TABLES

1 INTRODUCTION

In recent years, composite materials have been used in an increasing number of aerospace applications to reduce operating weight and cost by tailoring the material's high specific strength and stiffness for structural efficiency. Both military and commercial applications require strong and sound joining of composite materials. Traditionally, aircraft structural components have been joined by mechanical fastening, sometimes combined with adhesive bonding. More recently, some co-cured composite joints have incorporated z-pins, small pultruded carbon rods, through the joint to replace the traditional mechanical fastener. Z-pins have been shown to provide extra resistance to crack growth through composite joints without the added weight and complexity of mechanical fasteners[i-vi]. The Air Force Research Laboratory (AFRL) has conducted research on the use of z-pins in the co-bonding process using a new stubble approach.

1.1 Adhesive Bonding

Adhesive bonding is a structurally efficient method to join polymer matrix composites. It offers many advantages over mechanical fastening by eliminating the need for holes and by reducing the part count, cost, weight, and volume. Also, the applied loads are distributed more evenly along the surface which reduces the stress concentration. Bonding will likely be used in a broader range of aircraft applications as improvements are made to materials, process control, and inspection techniques. However, some structural joint applications with high pull-off requirements might require higher out of plane joint strength than an unreinforced bonded joint can offer. For instance, ballistic impacts on wet structure result in very high pull-off conditions due to hydrodynamic ram. One potential solution to these high pull-off conditions is z-pinned composite joints.

1.2 Co-curing with Through-Thickness Z-pins

The current method for using z-pins in the aerospace industry is to insert the pins through both members of a joint before the composite is cured, essentially nailing the pieces together. This requires that the structure be cured together with the z-pins already in place. There are times when the manufacturer would prefer not to co-cure since it could involve expensive, complex tooling and result in a higher number of defects, especially in orthogonal joints. In these cases they would prefer to co-bond or secondarily bond the structure.

1.3 Co-bonding with Z-pin Stubble

Co-bonding is the process of making composite joints with one or more parts already completely cured and one or more parts uncured. Some possible benefits of co-bonding are simpler, less expensive tooling and fewer defects in orthogonal joints. AFRL conducted preliminary research in previous programs using a z-pin joining process that is compatible with co-bonding. The first step in the process was to completely cure one component of a composite joint with z-pins through the thickness and extending beyond one surface. The region of pins that extends beyond the surface is called "stubble". However, this study was not matured to a level where the manufacturers would be willing to use it in designing or manufacturing airframes. The maximum stubble length previously obtained was 0.030 inch which barely penetrates the second composite adherend in the joint. Whereas this length still provides added strength to the joint and is easier to

tool, it does not offer the same advantages as a co-cured bond with pins that penetrate the full depth of the joint.

1.4 Research Objective

The objective of this research and development program was to develop and demonstrate a composite structural joint concept that incorporates z-pins but can be co-bonded instead of co-cured. The program developed the z-pin stubble concept by fabricating and testing double cantilever beam specimens with various stubble lengths and densities. These specimens were fabricated using novel ultrasonic insertion techniques. The previous limitation for stubble was 0.030 inch long and 2% aerial density. The technical challenge was to obtain full depth penetration with 4% aerial density.

2 MATERIALS AND MANUFACTURING

2.1 Materials – Composite, Z-Pins, and Peel Plies

The composite panels used in this study were created through hand lay-up. Two types of lay-ups have been utilized: 24 ply quasi-isotropic panels and 18 ply unidirectional panels, both made from AS4/3501-6 graphite epoxy. AF191 epoxy film adhesive was used on the peel ply screening co-bonded DCB specimens with a quasi-isotropic lay-up, but no adhesive was used on the unidirectional co-bonded DCB specimens. The Z-Fiber™ used in this program had a diameter of 0.020 inch and was nominally 0.6 inch long[vii], as shown in Figure 1.

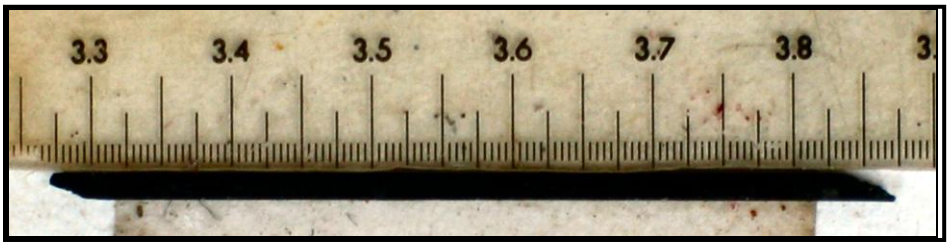

Figure 1: Photograph of Z-Fiber™

Additionally, a screening of peel ply materials and surface preparation techniques was conducted to evaluate the ability to remove the peel ply from the composite and the surface quality for bonding. Several different materials have been used as peel plies in the composite industry. AFRL conducted the screening test using four of the most common peel plies as well as other common laboratory materials. Z-pin stubble panels were fabricated with overall dimensions of 6 inch by 6 inch with a stubble field of 3 inch by 3 inch centered on the panel. The responses that were measured included:

1) ease of removal from the stubble field,
2) fabric contamination left on the z-pins, and
3) surface roughness.

Table 1 lists the materials that were used in the peel ply trials. A total of 12 trials were conducted, but some of the peel plies were similar. The materials that weren't already in stock were acquired from Airtech, a distributor of composite fabrication supplies.

Table 1: Materials Used for Peel Ply Screening

Material	Trade name	Thickness (in)
lon	Release Ply A	0.005
Nylon	Release Ply Super A	0.010
Nylon	Unknown	0.005
Coated nylon	Bleeder Lease B	0.006
Coated 7781 fiberglass	Bleeder Lease C	0.014
Teflon coated fiberglass	TFMP 200	0.003
Polyester	Release Ply Super G	0.007
Kevlar	Style 57017	0.006
High temperature material	Unknown	0.005
Extruded nylon bagging film	COEX VAC PAC 6262	0.003
Kapton	Unknown	0.004
Non-silicone rubber	Airpad	0.085

Table 2 shows that nylon, fiberglass, Kevlar, and polyester leave relatively the same roughness on the composite surface after removal. The nylon bagging film left a very smooth surface, and both Kapton and non-silicone rubber could not be removed from the surface.

Table 2: Peel Ply Trial Results

Peel Ply	Ease of Removal	Fabric Contamination	Surface Roughness
Nylon	Easy to remove	Left a few fibers	300 – 400 μin
Fiberglass	Very difficult to remove	Left a large number of fibers	100 – 200 μin
Kevlar	Very difficult to remove	Pulled some pins out but left no fibers	200 – 300 μin
Polyester	Very easy to remove	Came off cleanly	200 – 300 μin
Nylon Bagging Film	Difficult to remove	Came off cleanly	10 – 30 μin
Kapton	Could not remove in one piece	Film remained	n/a
Non-silicone Rubber	Could not remove in one piece	Rubber remained	n/a

A close up view of the surface texture can be seen in Figure 2. Each peel ply material left a unique pattern on the surface of the composite.

Figure 2: Photographs Of Surface Texture Left By Each Peel Ply

Figure 3 shows photographs of the stubble field for each of the peel plies. It can be seen that a slightly different texture is left for each material, some z-pins pulled out of the composite panel when the peel ply was removed, and peel ply fibers remained on the z-pin stubble for some of the trials.

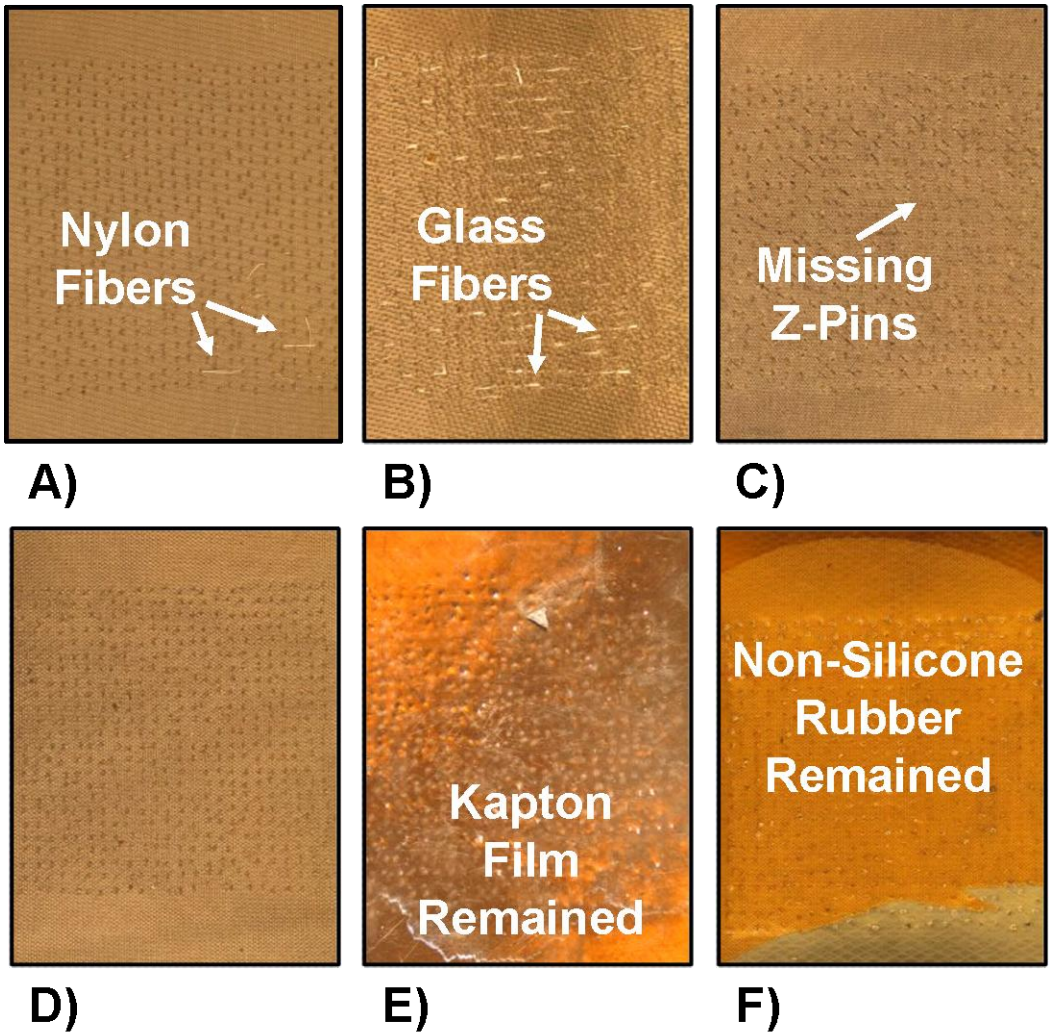

Figure 3: Photographs Of Z-Pin Stubble Fields For Trials Using Various Peel Plies Including: A) Nylon, B) Fiberglass, C) Kevlar, D) Polyester, E) Kapton, and F) Non-Silicone Rubber

Following the peel ply screening, the four most common peel plies (nylon, fiberglass, Kevlar, and polyester) were characterized in the new stubble fabrication process using double cantilever beam tests. The variables that were examined were peel ply material, stubble length, and surface preparation.

2.2 Manufacturing with Peel Plies

To develop and demonstrate a fail-safe adhesively bonded structural joint, a variety of fabrication trials and mechanical tests were performed. The composite, adhesive, and reinforcement all had to be prepared for fabrication and testing. Three basic groups of test specimens were created from the composite panels: unreinforced co-cured joints, unreinforced co-bonded joints, and Z-Fiber™ reinforced co-bonded joints. The Z-Fiber™ reinforced co-bonded joints were split into subcategories of different pin height, and each test group utilized the four peel plies and surface preparation techniques.

Similar manufacturing methods were employed to create the unreinforced co-cured joints and the unreinforced co-bonded joints. The co-cured test specimens were put together from two uncured panels whereas the co-bonded panels were assembled with one panel already put through a complete curing cycle in the autoclave according to the manufacturer's recommendation, and one uncured panel. Half of the cured panels were grit blasted in preparation for adhesive bonding using #180 alumina grit at a pressure of 40 psi and rinsed with acetone and blown dry with purified air. The initial crack length was created using 0.0005 inch thick Teflon film inserts between the panels. The peel ply material effect was determined using DCB specimens with an initial crack length of five inches while the stubble length effect specimens used a two inch initial crack. In the next step of fabrication, AF191 film adhesive was applied to the uncured panel; followed by placing both the cured and uncured panels together and debulking them. Once the panels had adhered sufficiently, they were vacuum bagged, and were autoclave cured using the AS4/3501-6 cycle as shown in Figure 4. To finalize production, the quasi-isotropic cured panels were cut to a length of 10 inches, the unidirectional panels to 8 inches, and both at a width of 1 inch using a diamond tip saw. To provide room for the test fixture pins, a hole was drilled through the specimen using a solid carbide drill bit. The final layout for the specimens is shown in Figure 5.

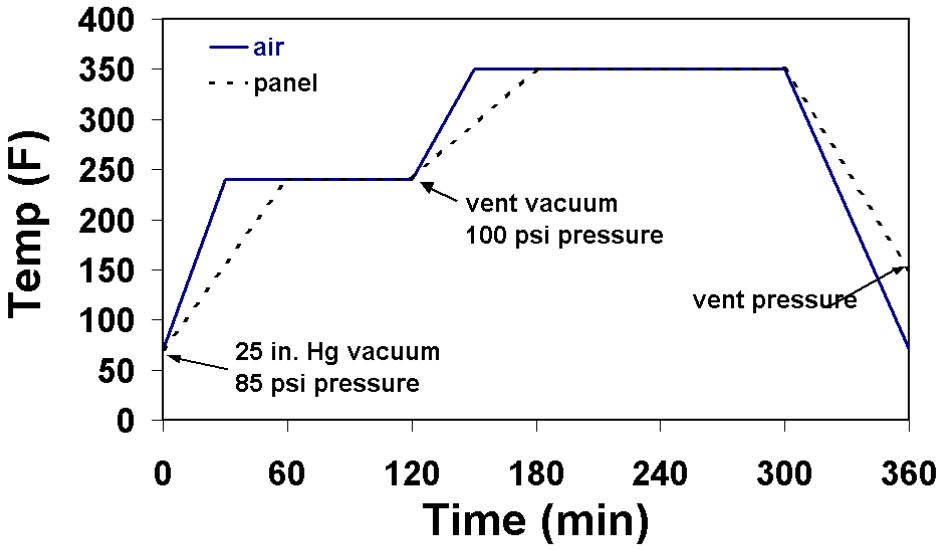

Figure 4: Cure Cycle for AS4/3501-6

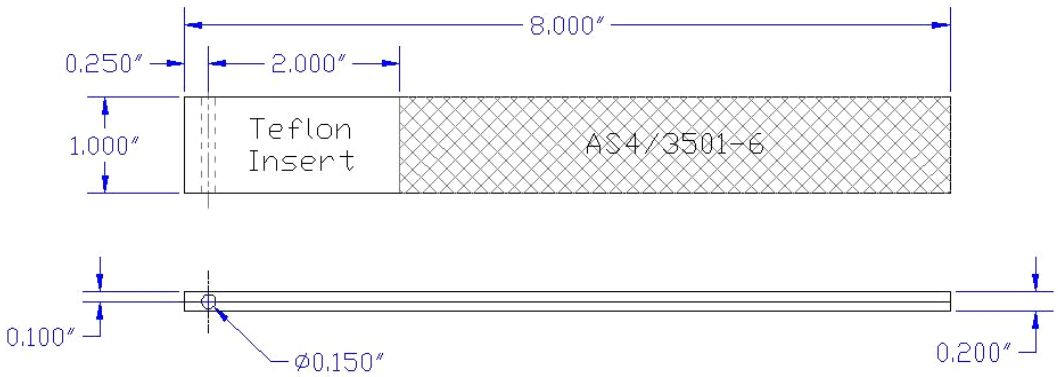

Figure 5: Unreinforced Co-Cured And Co-Bonded Test Specimens

The reinforced co-bonded test specimens were fabricated using two ultrasonic insertion steps as shown in Figure 6. First, multiple layers of appropriate cloth, usually nylon or polyester, are stacked on top of the peel ply and secured with Kapton tape to provide a surface for the z-pin stubble field on the uncured panel. This stack of cloth gives the appropriate height for the stubble as well as provides them with support during the autoclave cycle. Next, the z-pins were inserted ultrasonically through the thickness ("z" direction) and shaved off at the surface of the material stack. The panel is then cured and the peel ply and material removed. This leaves a field of stubble over the area of the joint. Adhesive and Teflon are applied to an uncured panel in the same method as used for the unreinforced joints described above. In later testing the adhesive was eliminated. The uncured panel is joined to the cured panel with the stubble field using ultrasonics once again. This ensures that the pins push all the way through the uncured laminate to create a strong joint. The panels are then put through another curing cycle, co-bonding them together. From this point they are cut and prepared for testing in the same manner as the unreinforced specimens. The final layout for the specimens is shown in Figure 7.

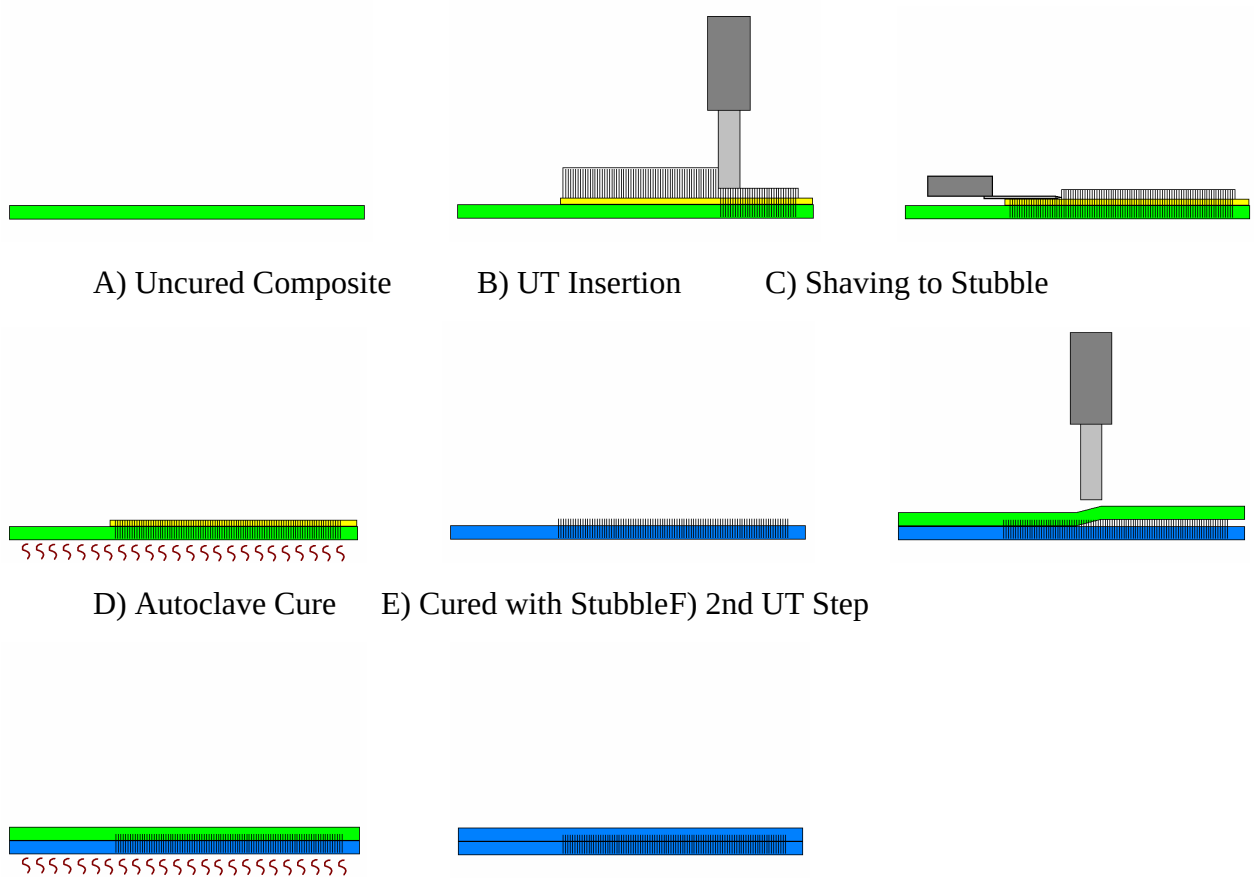

Figure 6: Novel Two-Step Ultrasonic Approach For Reinforcing Co-Bonded Composite Joints Using Z-Pin Stubble

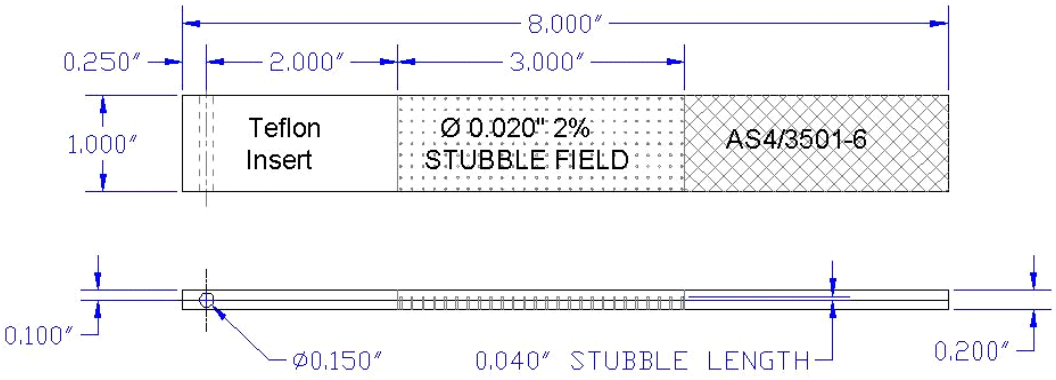

Figure 7: Reinforced Co-Bonded Test Specimens

The new process of using two separate steps of ultrasonic joining to create stubble reinforced joints was used to create DCB specimens as described below. Two separate stubble trials using peel plies were conducted during this study.

2.2.1 Stubble Lengths from 0.040 inch to 0.080 inch with Peel Ply

The first trial attempted to determine the effect of stubble lengths of 0.040 inch and 0.080 inch, stubble aerial densities of 2% and 4%, and pin diameters of 0.011 inch and 0.020 inch on the Mode I crack resistance. To create the stubble, alternating layers of polyester peel ply and non-porous Teflon were stacked to the desired height and taped to the composite surface with Kapton tape as shown in Figure 8 and Figure 9. The z-pins had diameters of 0.011 inch and 0.020 inch and original lengths between 0.5 and 1.0 inches. The DCB specimens in the first trial were made from 18 zero degree plies of AS4/3501-6 graphite epoxy prepreg tape (300 AW). They were a total of eight inches long, one inch wide, and two tenths inches thick. The initial two inch crack length was created by placing a 0.0005 inch thick sheet of Teflon in the mid plane of the specimen as shown in Figure 7.

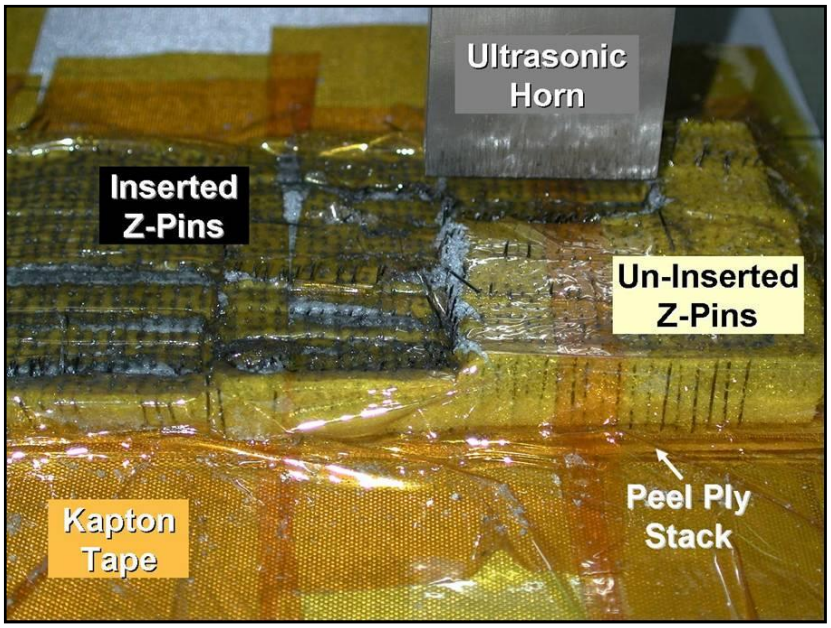

Figure 8: Ultrasonic Insertion of Z-Pins

Figure 9: Removal of Polyester Peel Ply and Non-Porous Teflon from Stubble

2.2.2 Stubble Lengths from 0.080 inch to 0.250 inch with Peel Ply

The second trial attempted to develop a manufacturing process to increase the stubble length from 0.080 inches to 0.250 inches. The stubble panels were fabricated from 50 zero degree plies of AS4/3501-6 graphite epoxy tape (150 AW). Similar to the first trial, a stack of polyester peel plies and non-porous Teflon was used to create the stubble height of 0.250 inches. Both 0.011 inch and 0.020 inch diameter z-pins were used in trial two. During the insertion process, the 0.020 inch diameter at 2% and 4% and the 0.011 inch diameter at 2% appeared to insert smoothly. The 0.011 inch diameter pins at 4% at both heights did not work the first time it was attempted. Figure 10 shows the initial attempt of inserting. The panel was redone and failed to insert properly the second time as well. The pins would go through the material stack easily but buckle as soon as they hit the composite surface. This failure may be due to the fact that the smaller diameter pins have less stiffness or that because of the larger height, the ultrasonic energy may not be reaching the surface of the composite.

After cure, the material stacks were removed. As more plies and Teflon were taken off it became apparent that many of the pins did not reach the surface of the composite or did not penetrate the full depth of the panel. Many pins were pulled out or broken when the peel ply materials had been completely removed. Figure 11 shows the extent of missing or malformed pins. Due to the amount missing, uneven stubble length, and malformation, a top panel could not be ultrasonically pressed onto this set of specimens.

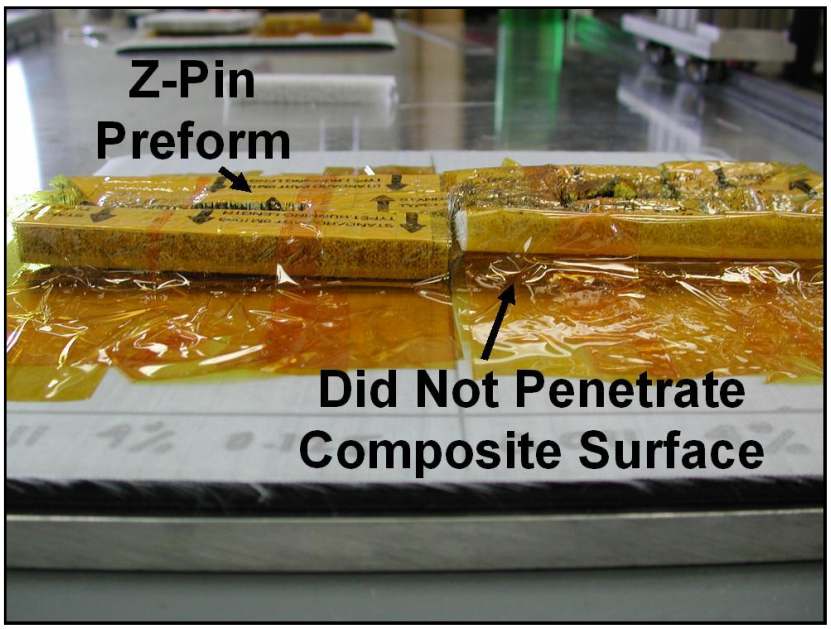

Figure 10: Photograph Showing the Failure of the Z-pins to Fully Insert into the Composite

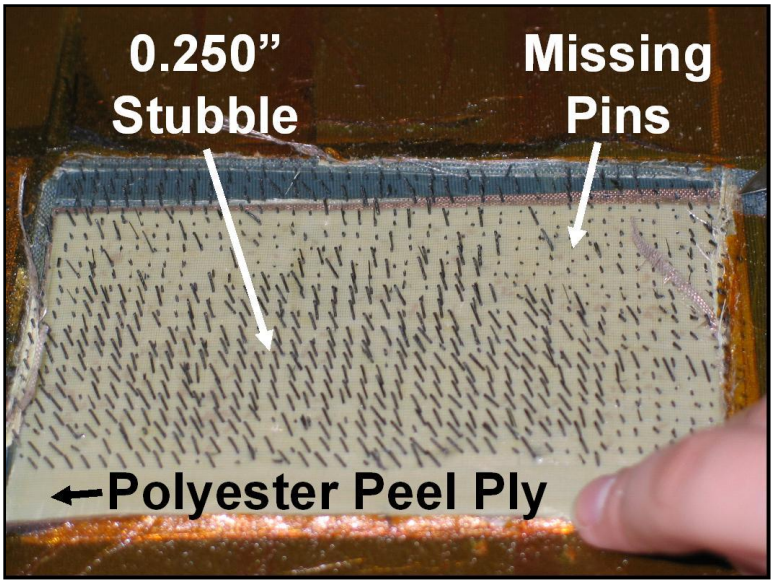

Figure 11: Photograph of Stubble Region after Partial Removal of Peel Ply Stack

2.3 Manufacturing with Rubber Sheets

Next, a variety of 0.125 inch thick rubber sheet materials were obtained from McMaster Carr for evaluation as a sacrificial material for stubble fabrication. Table 3 displays the material name, McMaster-Carr stock number, and some material properties of each of the rubber materials used for stubble fabrication. The most common types were variations of silicone, neoprene, and Buna-N. Additional information can be found from McMaster-Carr[viii]. Each of these materials were cut into four inch by four inch squares and placed in the center of a six inch by six inch composite panel section. A three inch by three inch region of z-pins were inserted through the center of the

rubber square and trimmed down to the surface of the rubber sheet as shown in Figure 12 and Figure 13. After cure, the rubber sheet was removed using a universal testing machine as shown in Figure 14. The entire four inch wide edge of the material was gripped and removed at a rate of 0.25 inch per minute for the first inch and at a rate of one inch per minute for the last three inches.

Table 3: Rubber Sheet Materials Used for Stubble Fabrication

Rubber Sheet Material Description	McMaster Carr Stock Number	Durometer (Shore A)	Tensile Strength (psi)	Stretch Limit (%)	Density (pcf)	Max Use Temp (F)
FDA-Compliant Silicone Foam	87485K42	-	100	300	35	450
Natural Gum	8633K54	40	3000	600	60	140
Silicone	8632K34	50	600	175	74	500
Commercial-Strength Neoprene	9455K624	60	1000	300	83	200
Elastic Natural Gum Foam	8601K31	-	85	150	30	160
Ultra-Elastic Natural Latex	86085K102	40	3850	810	61	158
High-Strength Neoprene	8568K713	60	1500	350	81	220
Commercial-Strength Buna-N	8635K564	60	900	200	84	170
Weather-Resistant EPDM	8610K84	60	1000	300	87	225
Adhesive-Ready Neoprene	86015K13	60	900	300	84	170
Fiberglass-Reinforced Silicone Sponge	85725K32	-	180	-	35	500
Red FDA Buna-N	8649K63	55	1200	500	84	200
Ozone-Resistant Hypalon	8618K15	65	1500	250	84	250
Air-Tight Butyl	8609K35	60	1500	300	84	225
White FDA Buna-N	86795K23	60	1000	350	84	180
General Purpose SBR	8634K42	75	700	150	86	170
Nylon-Reinforced High-Strg Neoprene	8599K33	70	1500	250	-	200
High-Strength Buna-N	86715K304	60	1500	300	78	200
Weather-Resistant EPDM Foam	86005K51	-	50	325	35	450
FDA Vinyl/Buna-N	8615K84	70	2000	400	90	220
Santoprene Thermoplastic Elastomer	86295K24	80	1050	410	-	500

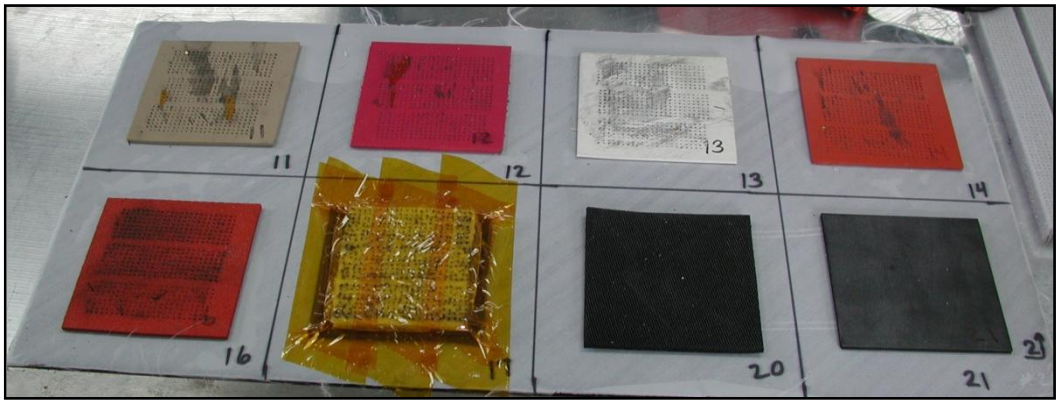

Figure 12: Composite Panel with Eight Stubble Trials Using Rubber Sheet Materials

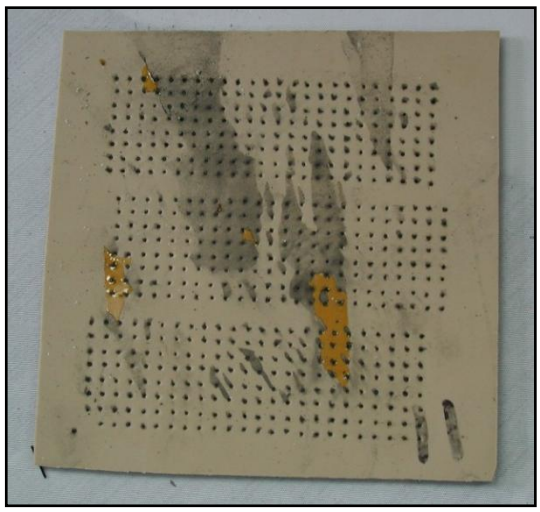

Figure 13: Rubber Sheet after Trimming Z-Pins

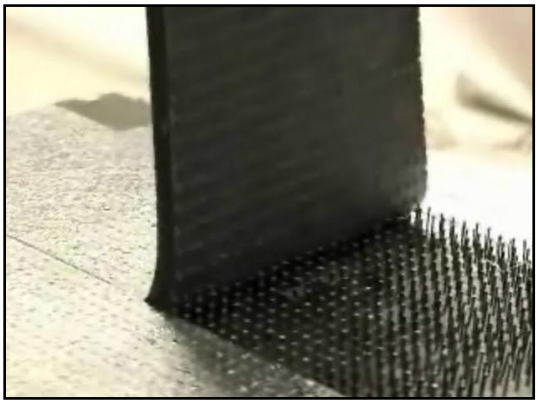

Figure 14: Rubber removal via MTS machine

2.3.1 Rubber Sheet Material Evaluation

The rubber sheet materials listed in Table 3 were evaluated based on (1) ease of pin insertion through the peel ply, (2) ability to trim pins to surface of peel ply material, (3) maximum pull-off load during removal of peel ply after cure, (4) quantity of pins remaining in the composite after peel ply removal, and (5) ability of peel ply material not to tear and slip out of the grips during removal.

Table 4 shows the materials that were tested and how they scored for each evaluation criterion. A score of 0 (red) was given if the material was found to be unacceptable for a given criterion. A score of 1 (yellow) was assigned if the material was determined to be acceptable. A score of 2 (green) was assigned of the material was excellent. For the overall evaluation, out of 21 materials, five were found to be excellent, six were found to be acceptable, and ten were found to be unacceptable. Each material was assigned an overall rating equal to the lowest rating in each of the five criteria.

Table 4: Rubber Sheet Materials Evaluation

Material Description	Pin Insertion	Pin Trim	Max Pull-off Load	Pins intact	Rubber material intact and gripped	Total Score
Silicone	2	2	2	2	2	10
Commercial-Strength Neoprene	2	2	2	2	2	10
High-Strength Neoprene	2	2	2	2	2	10
Commercial-Strength Buna-N	2	2	2	2	2	10
Weather-Resistant EPDM	2	2	2	2	2	10
Natural Gum	1	2	2	2	2	9
Adhesive-Ready Neoprene	2	1	2	2	2	9
FDA-Compliant Silicone Foam	2	1	2	1	2	8
Ultra-Elastic Natural Latex	1	2	2	2	1	8
Red FDA Buna-N	1	1	1	2	2	7
Ozone-Resistant Hypalon	1	1	1	2	2	7
Elastic Natural Gum Foam	2	1	2	2	0	7
Fiberglass-Reinforced Silicone Sponge	2	2	2	0	1	7
Air-Tight Butyl	2	2	1	2	0	7
High-Strength Buna-N	2	2	0	2	1	7
White FDA Buna-N	2	2	1	2	0	7
FDA Vinyl/Buna-N	2	1	0	2	2	7
General Purpose SBR	2	2	0	2	1	7
Santoprene Thermoplastic Elastomer	2	2	0	2	0	6
Weather-Resistant EPDM Foam	2	1	0	1	0	4
Fabric-Reinforced High-Strg Neoprene	0	0	0	0	1	1

2.3.2 Pin Insertion

The first evaluation criterion was the ease of pin insertion through the peel ply. Only one material was rated unacceptable (red) under this criterion. During pin insertion through the fabric-reinforced high strength neoprene rubber the pins had difficulty penetrating the material. Several pins eventually crushed under the ultrasonic load while others bent over. Four other materials were rated acceptable (yellow) but not excellent (green). During insertion through these materials, the tendency was for the z-pins to poke through the Kapton tape that held them down. Some pins completely popped out of the preform and failed to insert into the composite. Overall, the loss of pins was less than 5% so the ranking was acceptable.

2.3.3 Pin Trim

The second evaluation criterion was the ability to trim the pins to the surface of the peel ply material. Again, only one material was rated unacceptable under this criterion. While trimming the pins on the fabric-reinforced high strength neoprene, many full length pins completely popped out of the rubber sheet and failed to insert. Seven materials were rated acceptable (yellow). Two reasons for a yellow rating were (1) some pins popped out during trim and (2) rubber surface was damaged. Most of the rubber surfaces were durable enough to withstand the trimming process, especially with one layer of Kapton tape on top of the surface.

2.3.4 Maximum Pull-Off Load

The third evaluation criterion was maximum pull-off load during removal of the peel ply from the cured panel. This criterion was the largest overall discriminator. The peel ply removal loads were measured on a universal testing machine. Since peel plies are commonly removed by hand, easy removal is desired. An excellent rating (green) was given for materials with average pull-off loads

below 30 lb. An acceptable rating (yellow) was given for materials with average pull-off loads between 30 and 50 lb. An unacceptable rating (red) was given for materials with average pull-off loads greater than 50 lb. Table 5 shows each material's rating and the maximum load required to remove the rubber sheet from the stubble. Eleven materials received an excellent rating, four materials received an acceptable rating, and six materials received an unacceptable rating. Figure 15 shows the load-displacement plot for some of the typical rubber material removals.

Table 5: Rubber Removal Pull-Off Loads

Rubber Sheet Material Description	Avg Load (lb)
FDA-Compliant Silicone Foam	9
Natural Gum	15
Silicone	17
Commercial-Strength Neoprene	16
Elastic Natural Gum Foam	21
Ultra-Elastic Natural Latex	21
High-Strength Neoprene	22
Commercial-Strength Buna-N	27
Weather-Resistant EPDM	28
Adhesive-Ready Neoprene	28
Fiberglass-Reinforced Silicone Sponge	28
Red FDA Buna-N	33
Ozone-Resistant Hypalon	35
Air-Tight Butyl	43
White FDA Buna-N	44
General Purpose SBR	54
Nylon-Reinforced High-Strg Neoprene	66
High-Strength Buna-N	69
Weather-Resistant EPDM Foam	67
FDA Vinyl/Buna-N	88
Santoprene Thermoplastic Elastomer	96

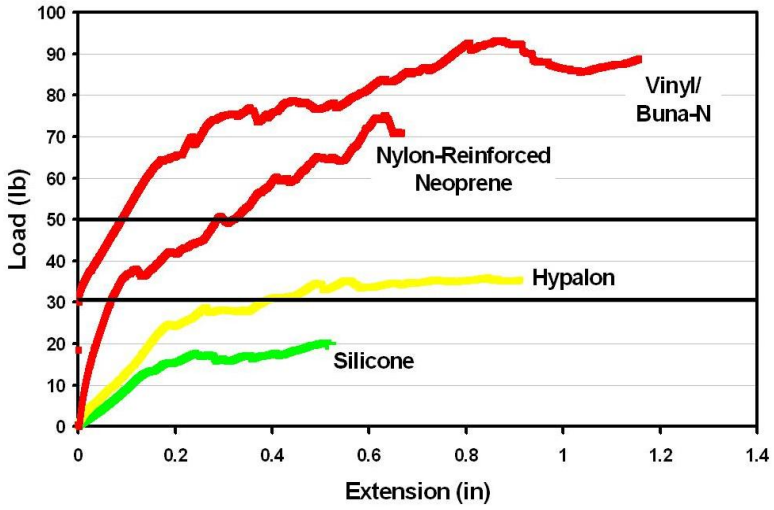

Figure 15: Typical Load-Displacement Plots of Rubber Sheet Removal from Stubble

2.3.5 Pins Intact

The fourth evaluation criterion was quantity of pins remaining in the composite after peel ply removal. Only two materials received an unacceptable rating. They were the fiberglass reinforced silicone sponge rubber and the fabric reinforced high strength neoprene. The pins tended to remain in the fabric reinforced materials rather than in the composite panel. The two materials that received an acceptable rating were foam rubbers which pulled a small percentage of pins out of the composite. The rest of the materials left all of the pins intact in the composite.

2.3.6 Rubber Material Intact and Gripped

The final evaluation criterion was ability of peel ply material not to tear and slip out of the grips during removal. Five materials received an unacceptable rating including: natural gum foam (ripped), EPDM foam (ripped), Santoprene (ripped), butyl (slipped out of grips), and white Buna-N (slipped out of grips). Five materials also received an acceptable rating as shown in Table 4. These materials left some debris on the stubble region but remained intact.

2.3.7 Successful 0.125 inch Stubble Fabrication

The rubber material evaluation was very successful in identifying a range of materials for stubble fabrication. Figure 16 shows a photograph of a stubble panel fabricated with 0.125 inch thick rubber. Clearly, all pins are intact, straight, and of a consistent height. The panel in Figure 16 shows that the fabrication challenge in Figure 11 was overcome.

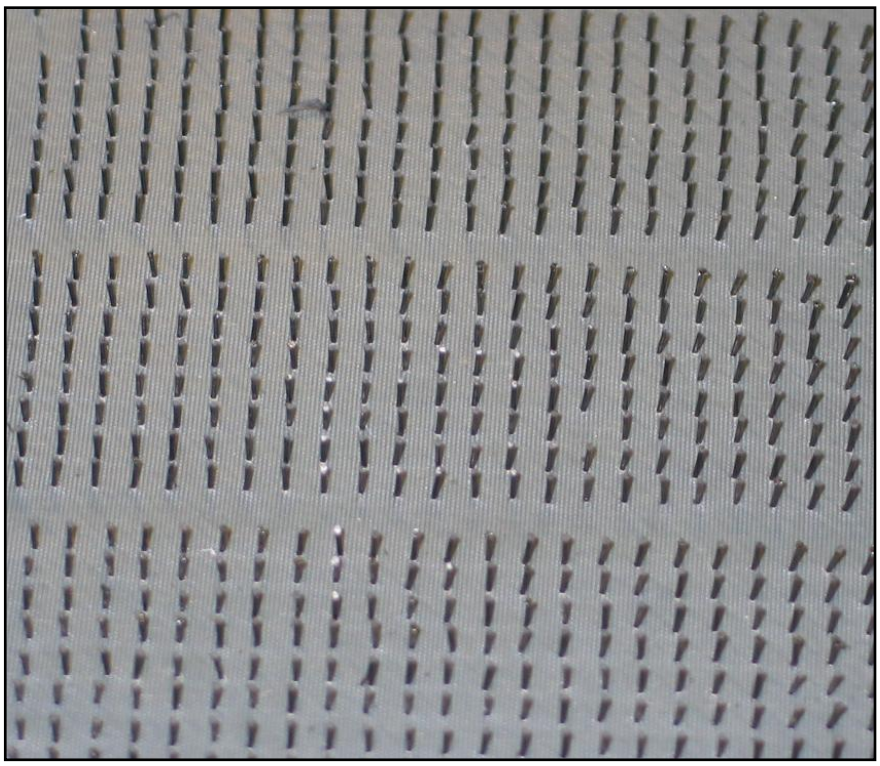

Figure 16: Photograph of Stubble Region after Removal of Rubber Sheet

2.3.8 Rubber Material Guidelines

During this study, the authors determined some optimum ranges of material properties when selecting a rubber sheet material for stubble fabrication. The following recommendations are provided to avoid problems during pin insertion, trim, and rubber sheet removal:

- Use material with durometer measurement less than or equal to 60 (Shore A) to avoid high pull-off loads.
- Use material with density greater than or equal to 60 pcf to avoid damage during trim.
- Avoid fabric reinforced materials since they tend to pull pins out of the composite.
- Use materials with tensile strengths greater than or equal to 100 psi to avoid ripping the material during removal.

2.3.9 Stubble-Reinforced DCB Specimens Using Rubber Sheets

Next, the new process of using two separate steps of ultrasonic joining to create stubble reinforced joints with rubber sheet material was put into practice. Stubble trials were conducted with 0.020 inch diameter z-pins to determine the effect of 0.125 inch and 0.250 inch long z-pin stubble and 2% and 4% stubble aerial densities on the Mode I crack resistance. Commercial strength neoprene was used as the sacrificial material to create the z-pin stubble fields since Table 4 showed that it exhibited excellent performance, and it was relatively inexpensive. The z-pins that were used had a diameter of 0.020 inch and original lengths of 0.475 and 0.875 inches.

Each side of the DCB specimen was fabricated from 28 zero degree plies of AS4/3501-6 graphite epoxy prepreg tape (300 AW). Each specimen was a total of ten inches long, one inch wide, and 0.6 inches thick. The initial four inch crack length was created by placing a 0.0005 inch thick sheet of Teflon in the mid plane of the specimen as shown in Figure 17. Since a smooth rubber sheet was used to create the z-pin stubble field, the stubble surface was grit blasted with glass beads and thoroughly rinsed with acetone after the first cure cycle to provide an appropriate surface for co-bonding the second composite.

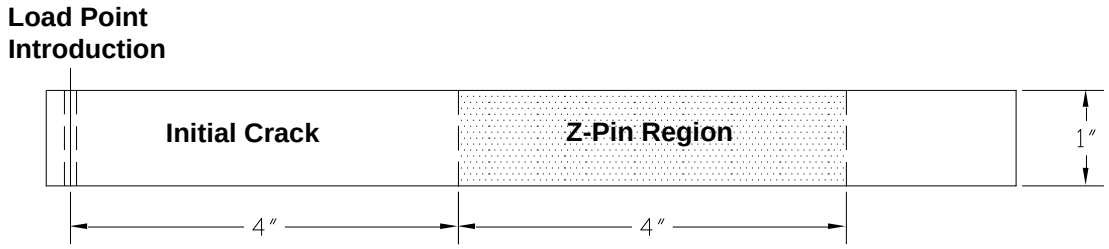

Figure 17: Schematic of Double Cantilever Beam Specimen

To achieve co-cured panels equivalent to 0.125 and 0.250 inch long co-bonded stubble, twelve inch by twelve inch sub-panels were assembled to the appropriate z-pin thicknesses (0.250 and 0.500 inches) with Teflon at the mid-plane as a crack-starter. Z-pins were then ultrasonically inserted through the entire thickness of the sub-panels which resulted in z-pins on each side of the mid-plane of lengths 0.125 and 0.250 inches. After the z-pins were inserted, additional plies were added to each side of the z-pinned panel to achieve the desired thickness of the specimen of 0.600 inches. This approach was successful in obtaining co-cured panels with z-pins of appropriate length on each side of the mid-plane. A schematic of the side-view of the co-cured specimen that is equivalent to the 0.125 inch long stubble specimen can be seen in Figure 18.

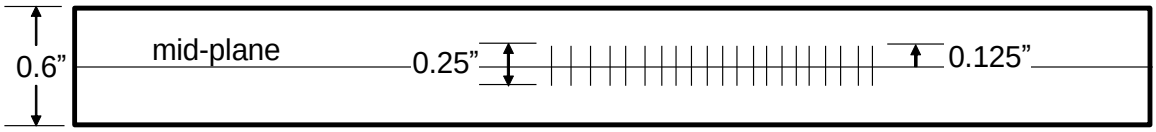

Figure 18: Schematic of Co-cured Z-pinned Baseline Specimen

Figure 19a shows a photograph of the successful fabrication of the 0.125 inch long stubble. Unfortunately, the 0.250 inch thick neoprene that was used to create 0.250 inch long stubble was difficult to remove in portions of the panel as shown in Figure 19b. As a result, only two specimens were extracted from the 0.250 inch stubble panel near the center where the neoprene came off cleanly. The portion of the panel with the neoprene residue was scrapped.

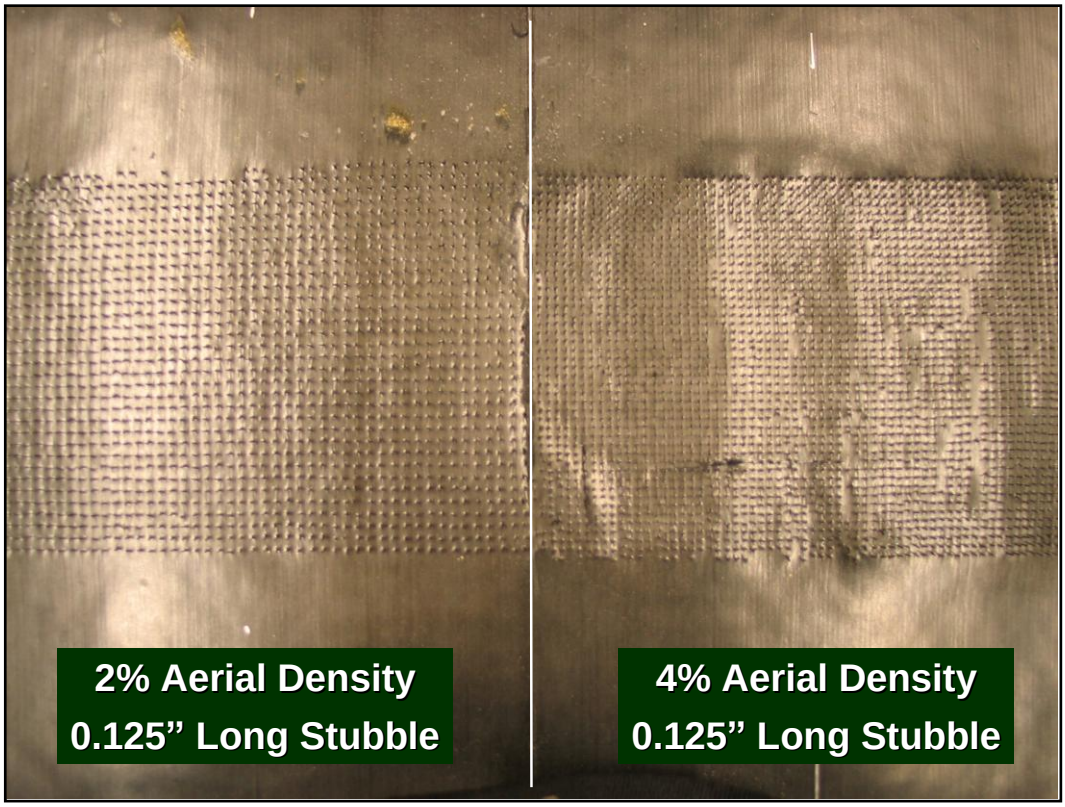
2% Aerial Density
0.125” Long Stubble
4% Aerial Density
0.125” Long Stubble

(a)

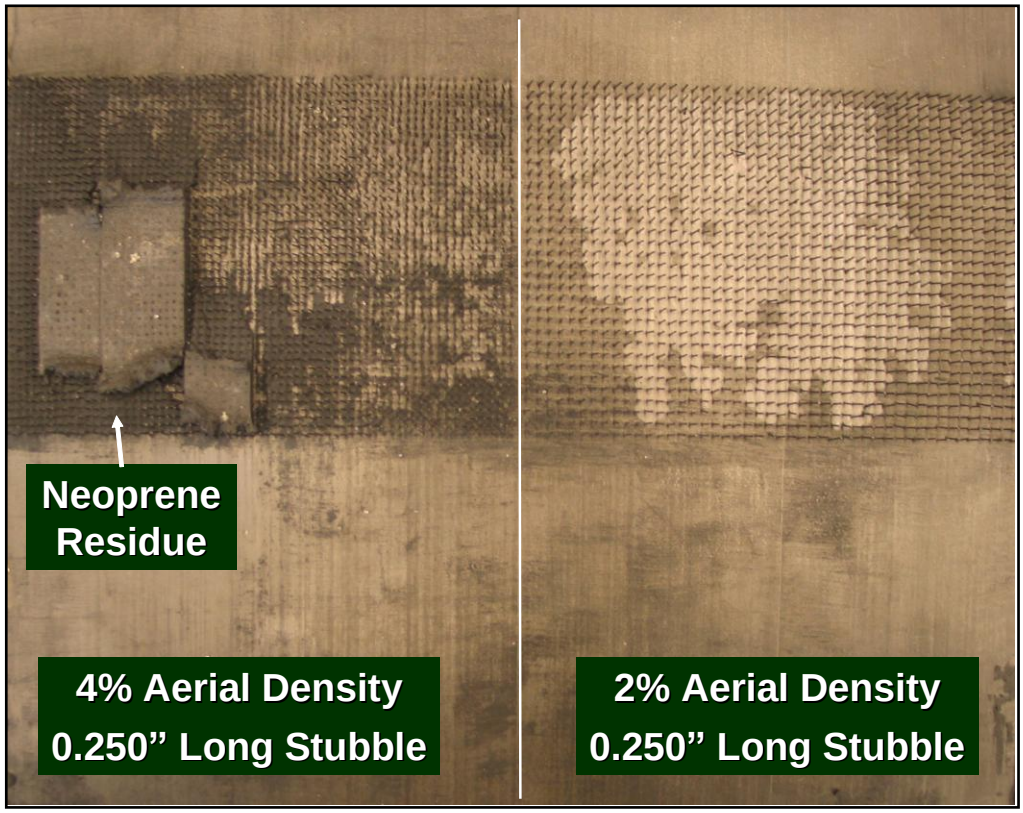

(b)

Figure 19: Photograph of 12” X 12” Stubble Panels after 1st Cure Cycle (a) 0.125” stubble (b) 0.250” stubble

3 EXPERIMENTAL DETAILS AND DATA REDUCTION

3.1 Modified Beam Theory

After the DCB specimens were fabricated they were tested on a MTS screw driven universal testing machine according to a modified ASTM D5528-94a procedure[ix]. The specimen is fixed onto the testing machine using a pin fixture, securing the specimen through the drilled holes. The specimen was loaded at 0.04 inches/minute until the crack grew to 0.25 inch at which point the rate was increased to 0.2 inches/minute. A microscope was used to observe the crack initiation and its progression through the joint. A modified beam theory[x] was used to analyze the fracture properties, while the critical energy release rate for initiation ($G_{ic\ initiation}$) was defined by the initial non-linearity in the energy release rate versus crack length curve. An average energy release rate value was determined for each specimen based on the area method.

During the double cantilever beam testing, the load and the load point displacement were measured. The actual crack extension as can be seen on one edge of the test specimen was also measured using a traveling optical microscope. These values, as well as several material properties were used to calculate the energy release rate.

The true fracture toughness of the laminate can be calculated from the unreinforced co-cured composite to composite DCB test. An "apparent" fracture toughness can be measured using a z-pin reinforced DCB test, but most research projects don't concentrate on this measurement. Instead, the unreinforced specimens are normally used to get the true fracture toughness and the reinforced specimens are used to calculate the interfacial shear strength of the z-pins. On the other hand, Cartie, et.al.[ii-v], of Cranfield University reported the "apparent" fracture toughness of reinforced composites in the open literature.

The ultimate goal of the DCB testing is to plot the load (P) versus load point displacement (δ) and the energy release rate (G) versus crack length (a). The area under the load – displacement plot generally describes an energy to break.

True fracture toughness of unreinforced composites can be calculated using Equations 1 and 2 below.

$$\textit{Load point displacement} = \delta = \frac{2P(a+\chi h)^3}{3E_{fx}I} + \frac{12P(a+\chi h)}{5G_{xz}hw} \qquad (1)$$

$$\textit{Mode I Energy Release Rate} = G_I = \frac{P^2}{w}\left[\frac{(a+\chi)^2}{E_{fx}I} + \frac{6}{5G_{xz}hw}\right] \qquad (2)$$

where

δ = load point displacement measured with the MTS crosshead displacement transducer
P = applied load measured with the MTS load cell and recorded in the data file
a = crack length calculated from the load measurement, displacement measurement, and the laminate compliance (see equation below)
χ = correction factor for crack tip elasticity (see Equations 3 and 4 below)
h = half specimen thickness
E_{fx} = flexural modulus calculated with load/displacement data and nominal laminate properties
I = moment of inertia = $wh^3/12$

G_{xz} = *nominal laminate transverse shear modulus*
w = specimen width

The correction factor for crack tip elasticity can be found using Equation 3:

$$\chi = \sqrt{\frac{E_{xx}}{11G_{xz}}\left\{3-2\left(\frac{\Gamma}{1+\Gamma}\right)^2\right\}} \tag{3}$$

$$\text{where } \Gamma = 1.18\frac{\sqrt{E_{xx}E_{yy}}}{G_{xz}}, \tag{4}$$

E_{xx} = *nominal laminate x-direction in-plane modulus*
E_{yy} = *nominal laminate y-direction in-plane modulus*
G_{xz} = *nominal laminate transverse shear modulus*

For AS4/3501-6 quasi-isotropic DCB specimens, the in-plane stiffness properties measured for 24 ply quasi AS4/3501-6 were:

E_{xx} = 7.9 x 10^6 psi
E_{yy} = 7.9 x 10^6 psi

The transverse shear modulus of quasi-isotropic AS4/3501-6 was found to be:

G_{xz} = 0.48 x 10^6 psi

Using these values, the correction factor for analysis of quasi-isotropic AS4/3501-6 is:

$$\Gamma = 1.18\frac{\sqrt{E_{xx}E_{yy}}}{G_{xz}} = 1.18\frac{\sqrt{\left(7.9\times10^6\,psi\right)\left(7.9\times10^6\,psi\right)}}{0.48\times10^6\,psi} = 19.4$$

$$\chi = \sqrt{\frac{E_{xx}}{11G_{xz}}\left\{3-2\left(\frac{\Gamma}{1+\Gamma}\right)^2\right\}} = \sqrt{\frac{7.9\times10^6\,psi}{11\left(0.48\times10^6\,psi\right)}\left\{3-2\left(\frac{19.42}{1+19.42}\right)^2\right\}} = 1.33$$

For AS4/3501-6 unidirectional DCB specimens, the in-plane stiffness properties for unidirectional AS4/3501-6 were:

E_{xx} = 22.9 x 10^6 psi
E_{yy} = 1.49 x 10^6 psi

A paper by James Reeder of NASA[xi] reported the transverse shear modulus of AS4/3501-6 to be:

G_{xz} = 0.85 x 10^6 psi

Using these values, the correction factor for analysis of unidirectional AS4/3501-6 was:

$$\Gamma = 1.18\frac{\sqrt{E_{xx}E_{yy}}}{G_{xz}} = 1.18\frac{\sqrt{(22.9\times10^6\ psi)(1.49\times10^6\ psi)}}{0.85\times10^6\ psi} = 8.11$$

$$\chi = \sqrt{\frac{E_{xx}}{11G_{xz}}\left\{3-2\left(\frac{\Gamma}{1+\Gamma}\right)^2\right\}} = \sqrt{\frac{22.9\times10^6\ psi}{11(0.85\times10^6\ psi)}\left\{3-2\left(\frac{8.11}{1+8.11}\right)^2\right\}} = 1.86$$

To calculate G_I, the flexural modulus (E_{fx}) was calculated using Equation 5 below:

$$E_{fx} = \frac{2(a_0+\chi h)^3}{3I} \Big/ \left[\frac{1}{m} - \frac{12(a_0+\chi h)}{5G_{xz}hw}\right] \quad (5)$$

where
a_0 = *initial crack length from Teflon insert*
χ = *correction factor for crack tip elasticity*
h = *half specimen thickness*
I = *moment of inertia*
m = *slope of linear fit to load versus load point displacement plot*
G_{xz} = *nominal laminate transverse shear modulus*
w = *specimen width*

The ultimate desire is plot the crack resistance curve: energy release rate (G) versus crack length (a). To do this, the crack length as a function of load and load point displacement must be calculated using the compliance of the laminate. These calculations can be verified by the crack length measurement made with the traveling optical microscope. Equations 6 and 7 can be used for this calculation.

$$a_{est} = \sqrt[3]{(3/2)E_{fx}IC} - \chi h \quad (6)$$

$$a = \sqrt[3]{(3E_{fx}I/2\left[C - \frac{12(a_{est}+\chi h)}{5G_{xz}hw}\right]} - \chi h \quad (7)$$

where
E_{fx} = *flexural modulus (see Equation 5)*
I = *moment of inertia*
χ = *correction factor for crack tip elasticity*
h = *half specimen thickness*
G_{xz} = *nominal laminate transverse shear modulus*
w = *specimen width*

$$C = \frac{\delta}{P} = \frac{V_P - V_{P\_Adjust}}{P}$$

where

V_P = measured load-point displacement

V_{P_Adjust} = displacement offset based on true zero-displacement intercept = $-P_0/m$

where P_0 = intercept and m = slope of linear fit

P = measured load

Once the crack resistance curve was plotted, the critical energy release rate (G_{IC}) was determined by the first nonlinearity from the initial vertical line.

Table 6 shows some of the input properties for the modified beam theory analysis. These values were obtained from experimental results using AS4/3501-6 laminates and from the open literature.

Table 6: Input Properties For Modified Beam Theory Analysis

	24 ply quasi-isotropic	18 ply unidirectional
E_{xx}	7.9 x 10^6 psi	22.9 x 10^6 psi
E_{yy}	7.9 x 10^6 psi	1.49 x 10^6 psi
G_{xz}	0.48 x 10^6 psi	0.85 x 10^6 psi

3.2 DCB Testing with 0.040 To 0.080 inch Stubble (Peel Ply)

As mentioned above, the first stubble experiments used peel plies for the sacrificial material during fabrication. These tests were conducted to increase the correlation range between stubble parameters and delamination resistance. The original test matrix included both 0.011 and 0.020 inch diameter pins and 2 and 4% aerial densities. Difficulty in stubble manufacturing limited the experiments to what is shown in Table 7.

Table 7: DCB Test Matrix for 0.040 to 0.080 inch Stubble (Peel Ply)

Original Plan			Revised Plan		
Pin Diameter (in)	Aerial Density (%)	Stubble Height (in)	Pin Diameter (in)	Aerial Density (%)	Stubble Height (in)
0.011	2	0.040	0.011	2	0.040
0.011	4	0.040	x	x	x
0.011	2	0.080	x	x	x
0.011	4	0.080	x	x	x
0.020	2	0.080	0.020	2	0.080
0.020	4	0.040	0.020	4	0.040
0.020	4	0.080	0.020	4	0.080

After the DCB specimens were fabricated, they were tested on a screw driven universal testing machine as described above. The experimental data was reduced according to the modified beam theory as shown in equations 1-7.

3.3 DCB Testing with 0.125 to 0.250 inch Stubble (Rubber)

DCB stubble experiments were conducted to increase the correlation range between stubble length and delamination resistance to include both 0.125 and 0.250 inch long stubble as well as 2 and 4% aerial densities. The entire test matrix is shown in Table 8.

Table 8: DCB Test Matrix for 0.125 To 0.250 inch Stubble (Rubber)

Aerial Density (%)	2nd Ultrasonic Step	Stubble Height (in)
2	Yes	0.125
2	Yes	0.250
2	No	0.125
2	No	0.250
4	Yes	0.125
4	Yes	0.250
4	No	0.125
4	No	0.250
2	Co-cured (baseline)	0.125
2	Co-cured (baseline)	0.250
4	Co-cured (baseline)	0.125
4	Co-cured (baseline)	0.250

The DCB specimens were tested on a screw driven universal testing machine as described above. It was found that the strength of the existing pin fixture was insufficient for the longer stubble fields. The loading pin and clevis both experienced permanent deformation due to the excessive loads during DCB testing of the 0.125 and 0.250 inch z-pin stubble specimens as shown in Figure 20a. The fixture was redesigned to accommodate higher loads as shown in Figure 20b. A second modification was done to more evenly distribute the load on the center plies of the DCB specimens as shown in Figure 20c.

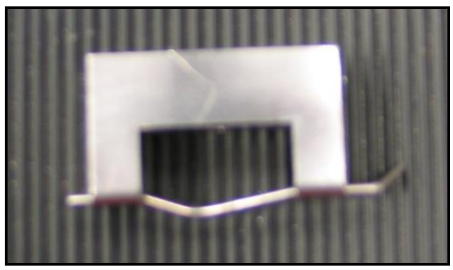

(a)

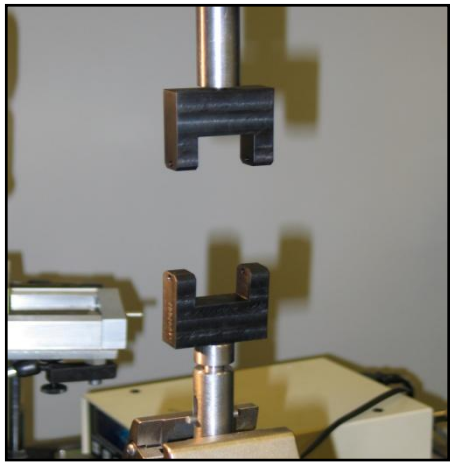

(b)

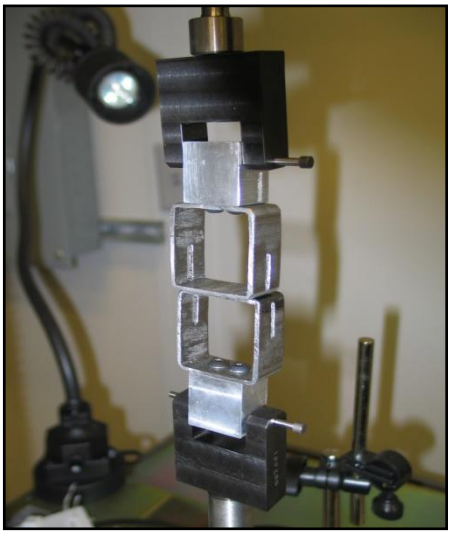

(c)

Figure 20: DCB Test Fixture (a) Original Failed Fixture, (b) First Mod, and (c) Second Mod

Using the new fixture as shown in Figure 21, the specimens were loaded at 0.04 inches/minute until the crack grew to 0.25 inch at which point the loading rate was increased to 0.2 inches/minute.

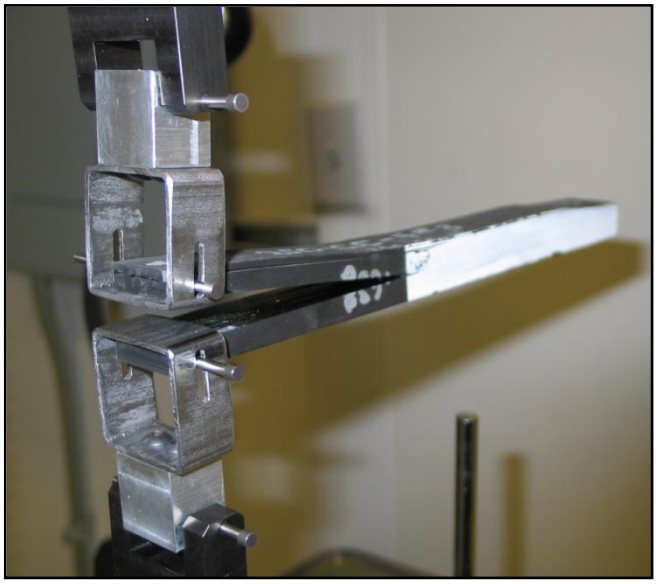

Figure 21: Photograph of DCB Specimen in Pin-Loaded Fixture

4 RESULTS

Two separate series of experiments were conducted in order to 1) characterize the effect of peel ply material and grit blasting on Mode I delamination toughness and 2) define the relationship between z-pin stubble length and delamination resistance of composite laminates reinforced with z-pin stubble.

4.1 Effect of Peel Ply Material and Grit Blasting on the Mode I Delamination Toughness

The first DCB tests were conducted to determine the effect of peel ply material and grit blasting on the Mode I delamination toughness of 24 ply quasi-isotropic AS4/3501-6 graphite epoxy. The co-cured baseline did not include adhesive in the joint, but the co-bonded DCB specimens contained one layer of AF191 film adhesive at the centerline of the joint. It should also be noted that difficulties arose during fabrication of the 0.080 in long stubble specimens. A non-silicone rubber pad (AirPad^{TM}) was used to create the z-pin stubble field. This rubber material was selected since it was available in the desired thickness. Once the stubble panel was cured, it was very difficult to remove the AirPad^{TM} from the stubble field. A large number of z-pins completely pulled out of the stubble panel and remained in the AirPad^{TM}. The panels were still used to fabricate DCB specimens in order to characterize the effect of missing pins. The following results clearly show that the missing pins have a very detrimental effect on the delamination properties.

The properties that were measured were the critical energy release rate for crack initiation, the maximum load obtained during Mode I testing, and the average energy release rate based on the enclosed area under the load – displacement curve. The data in the graphs are an average of four specimens tested at each condition, with the error bars showing one standard deviation.

Figure 22 shows the apparent G_{ic} for crack initiation. Several significant effects can be seen. First, the co-cured baseline without film adhesive has a much lower G_{ic} for initiation than the co-bonded specimens with AF191 film adhesive. In most cases, the G_{ic} for initiation went from less than one for the co-cured specimens with no adhesive to a value of three to four for co-bonded specimens with adhesive. It turns out that the film adhesive had such a large effect that no significant difference was seen for the four different peel ply materials or for the grit blasted surface prep on either the unreinforced or 0.030 inch z-pin stubble reinforced specimens. In fact, the adhesive toughness essentially made the 0.030 inch stubble of no effect with respect to G_{ic} for initiation. Another obvious discovery is that specimens fabricated with the AirPad^{TM} rubber performed very poorly in Mode I testing. The combination of missing pins and contaminated surface resulted in G_{ic}'s for initiation of less than 25% of the other specimens.

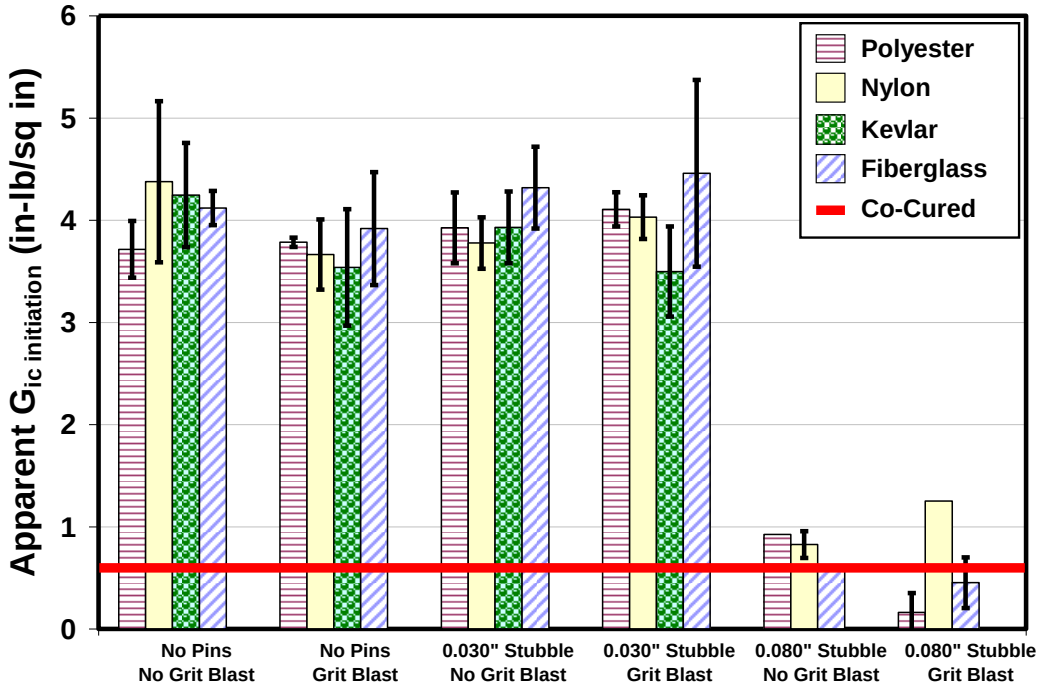

Figure 22: Effect of Peel Ply Material, Grit Blasting, and Stubble Length on the Apparent Gic for Crack Initiation for 24 Ply Quasi-Isotropic AS4/3501-6 with AF191 Film Adhesive

The maximum loads obtained during Mode I testing are shown in Figure 23. Similar to the previous discussion, the largest effect on the maximum load is the presence of a film adhesive in the joint. The maximum load for all peel ply materials, with and without grit blasting, and with and without 0.030 inch stubble all fell within the range of 15 to 20 pounds. One thing to note is that the specimens prepared with a polyester peel ply performed better without grit blasting. As was mentioned in the materials section of this paper, the polyester peel ply left a clean surface with no stray fibers remaining on the stubble. The grit blasting procedure was used to try to remove the glass fibers that remained on the stubble after the fiberglass peel ply was removed. Unfortunately, the fiberglass results don't show any improvement for the grit blasted specimens either. Finally, the effect of missing pins on the 0.080 in stubble was not as significant for the maximum load as it was for the G_{ic} for initiation.

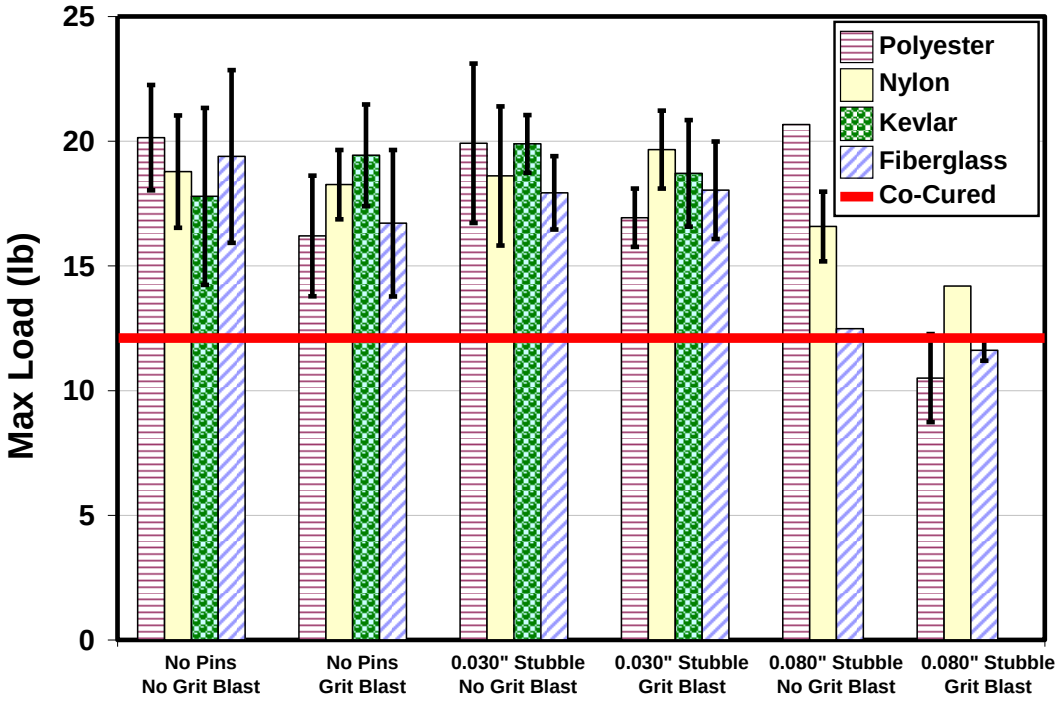

Figure 23: Effect of Peel Ply Material, Grit Blasting, and Stubble Length on the Maximum Mode I Load for 24 Ply Quasi-Isotropic AS4/3501-6 with AF191 Film Adhesive

The final analysis performed in the peel ply screening was the calculation of an average energy release rate using the area method. The initial crack length for these specimens was five inches. The enclosed area was calculated on each load - displacement curve from a five inch to a seven inch crack extension. The results presented in Figure 24 clearly show some benefits of z-pin stubble and grit blasting. It can be seen that grit blasting unreinforced DCB specimens significantly increases the average energy release rate. The results also indicate that the addition of 0.030 inch long z-pin stubble in the co-bonded joint significantly improves the energy release rate during crack propagation. In some cases the improvement obtained from the z-pin stubble is on the order of 10X to 100X. As expected, the true benefit of through-thickness reinforcement is demonstrated during crack propagation rather than crack initiation. It should also be noted that the average energy release rate for the co-cured specimens was relatively high compared to the co-bonded specimens. One possible reason for this observation is fiber bridging. It is likely that fiber bridging occurred for the co-cured tests and did not occur for the co-bonded tests. Recall that the co-bonding process involves completely curing one panel before joining the second uncured panel. Also, a film adhesive layer was placed in the co-bonded joint that would prevent fiber bridging from taking place. Finally, the 0.080 inch stubble specimens did not exhibit the extreme degradation in properties that was seen in the previous analyses. In this case, the fibers that remained were somewhat effective in increasing the crack resistance during propagation.

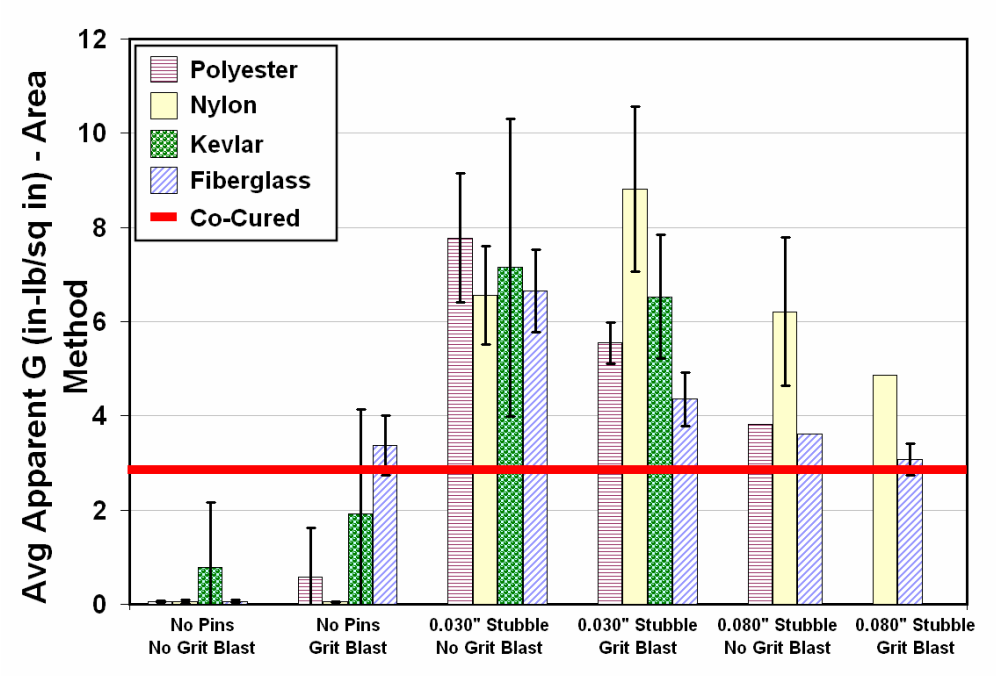

Figure 24: Effect of Peel Ply Material, Grit Blasting, and Stubble Length on the Average Energy Release Rate (Area Method) for 24 Ply Quasi-Isotropic AS4/3501-6 with AF191 Film Adhesive

4.2 Effect of Z-Pin Stubble Length on the Mode I Delamination Toughness

4.2.1 0.040" to 0.080" Stubble, 0.020" Diameter Pins, 2% Aerial Density

The next set of DCB tests were conducted to determine the effect of z-pin stubble length on the Mode I delamination toughness of 18 ply unidirectional AS4/3501-6 graphite epoxy. The z-pins used for this part of the research had a diameter of 0.020 inch and an aerial density of 2%. For this series of experiments, all of the specimens were co-bonded with no adhesive in the joint. A stack of polyester peel plies was used to fabricate specimens with 0.040 inch and 0.080 inch stubble lengths. Initial crack lengths of two and four inches were created using a 0.0005 inch Teflon film insert. It was determined that the two inch initial crack length produced more repeatable results than the four inch initial crack. Crack tip elasticity may have been an issue for the longer crack extensions. Therefore, only the results from the specimens with a two inch initial crack will be presented.

Figure 25 shows the load versus load point displacement for both the unreinforced and z-pin stubble reinforced DCB tests. These results graphically show the benefits of z-pin stubble in Mode I type loading conditions. The maximum load and area under the curve are obviously higher for the specimens with z-pin stubble. These will be quantified in subsequent graphs. It is also clear that the scatter in the data is small enough to clearly distinguish between the behaviors of each z-pin stubble condition.

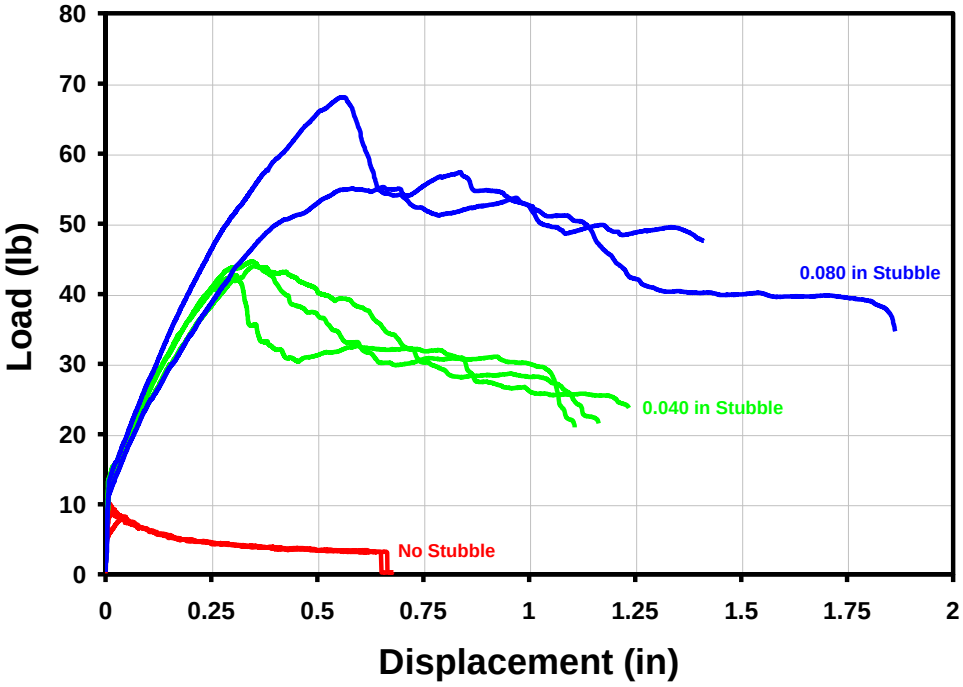

Figure 25: Effect of Z-Pin Stubble on the Mode I Load – Displacement Behavior for Co-Bonded 18 Ply Unidirectional AS4/3501-6 Graphite Epoxy with No Adhesive Layer

The resistance curves for the unreinforced and z-pin stubble reinforced specimens are shown in Figure 26. It is clear that the stubble length plays a significant role in the crack resistance behavior. The apparent energy release rates during crack propagation increase significantly with increasing stubble length. Also, it should be noted that the critical energy release rate for crack initiation was very difficult to determine for this data set. It appears that a crack started to grow at a slow rate at a relatively low load. The stubble reinforced G_{ic} for initiation was in the range of 0.75 to 1 in-lb/sq in, while the unreinforced value was determined to be in the range of 0.15 to 0.20 in-lb/sq in.

These results agree with previous studies reported in the open literature[ii-iv]. First, z-pinned laminates demonstrated only minimal improvements, if any, with respect to the G_{ic} for initiation. Second, it can be seen in Figure 25 and Figure 26 that the 0.040 inch and 0.080 inch long stubble started loading at the same rate, but the 0.080 inch long stubble specimens continued to increase in load after the 0.040 inch long stubble specimens began to decrease in load. This can be explained by the z-pin failure mechanism described by Liu, et.al.[xii], in which a bridging law is described. The pinned laminate goes through initial elastic debonding, unstable debonding, and finally frictional sliding. Figure 27 graphically shows that as a crack grows through a z-pin field, multiple rows of pins carry the load simultaneously and experience frictional sliding until the row of pins is completely separated from one of the adherends. The 0.080 inch long stubble pins begin to carry the same load as the 0.040 inch long pins until the first row of 0.040 inch long pins pull completely out of one side of the DCB specimen. At this point, the load carrying capacity levels off as a constant number of z-pin rows are active. Since the 0.080 inch long pins are embedded deeper in the laminate, a larger number of z-pin rows are active, as shown in Figure 27. Therefore, the load continues to increase until the first row of pins pulls completely out of

one adherend. It is expected that this relationship would continue to be true with increasingly longer pins, possibly up to a point in which the composite adherend would fail in bending prior to z-pin pull-out or the z-pins might actually fracture if the pins are long enough.

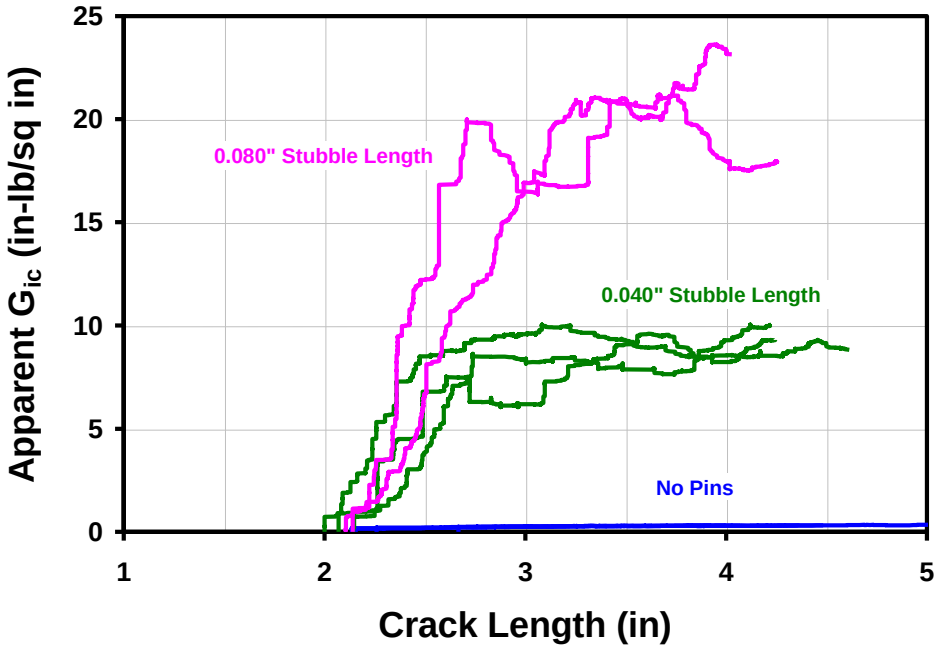

Figure 26: Effect of Z-Pin Stubble on the Mode I Energy Release Rate as a Function of Crack Length for Co-Bonded 18 Ply Unidirectional AS4/3501-6 Graphite Epoxy with No Adhesive Layer

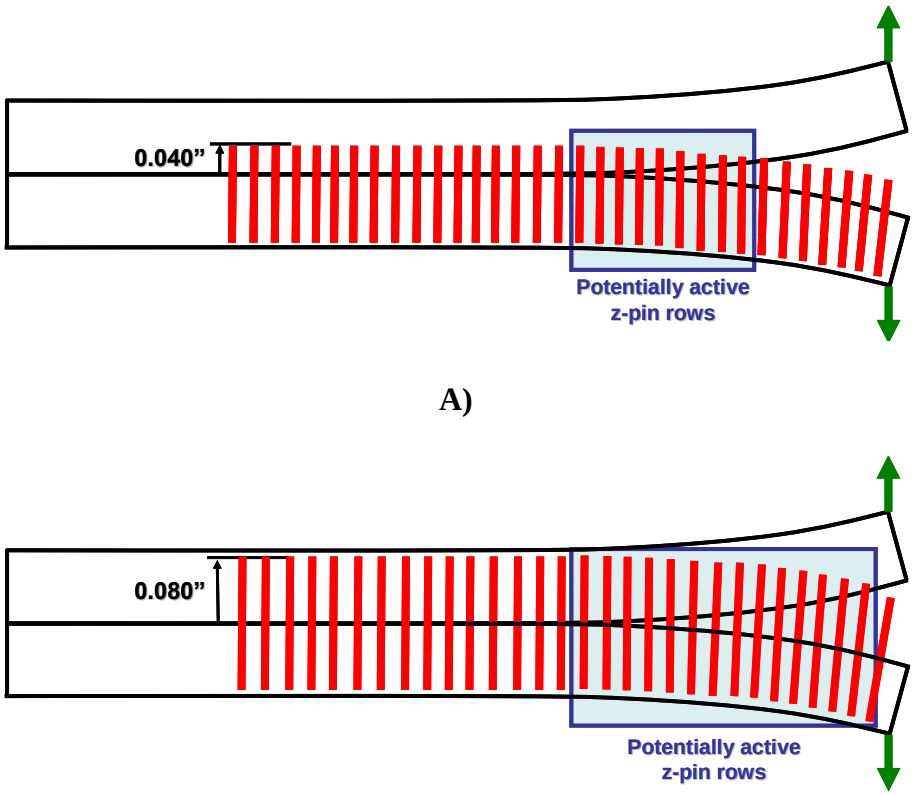

Figure 27: Schematic of Z-Pin Pull-out with Multiple Active Rows for A) 0.040 inch Stubble and B) 0.080 inch Stubble

The average maximum loads obtained in Figure 25 are plotted as a function of stubble length in Figure 28. Each data point is an average of three to four tests with the error bars representing one standard deviation. The z-pin stubble field dramatically increased the load carrying capability of the DCB specimen during crack propagation. The average maximum load for the unreinforced joint was 9.2 lb, while the 0.040 inch long stubble increased the maximum load to 43.9 lb, and the 0.080 inch long stubble increased it farther to a value of 63.7 lb. This corresponds to an increase of 4.8X and 6.9X for the 0.040 inch and 0.080 inch long stubble, respectively. The increased load is made possible by the frictional sliding load between the z-pins and the composite matrix.

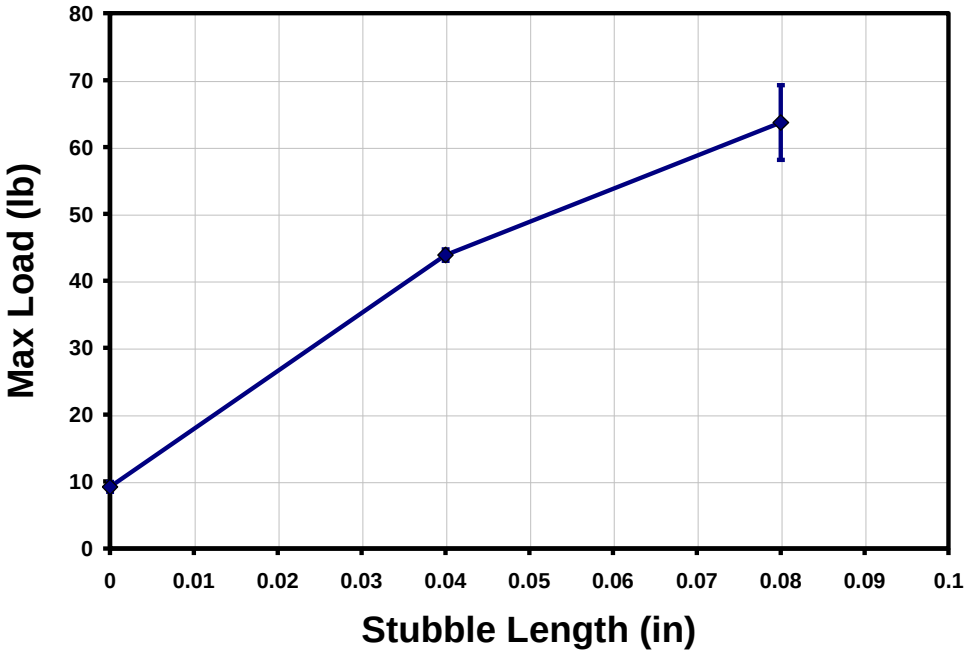

Figure 28: Effect of Z-Pin Stubble Length on the Maximum Load Obtained in Mode I Loading for Co-Bonded 18 Ply Unidirectional AS4/3501-6 Graphite Epoxy with No Adhesive Layer

All of these results are from specimens that were fabricated with a two inch initial crack. For comparison, the average apparent critical strain energy release rate at a crack extension of four inches is shown as a function of stubble length in Figure 29. A four inch crack was selected since all of the specimen configurations had fully achieved their plateau value by the time the crack had grown from two inches to four inches, as shown in Figure 26. The average G_{ic} went from 0.3 in-lb/sq in for the unreinforced specimens to 8.9 and 23.5 in-lb/sq in for the 0.040 inch and 0.080 inch long stubble, respectively. This corresponds to approximately a 30X to 80X increase. These results show that increasing the depth of the z-pin in the composite laminate makes a significant impact to the joint's delamination resistance during crack propagation.

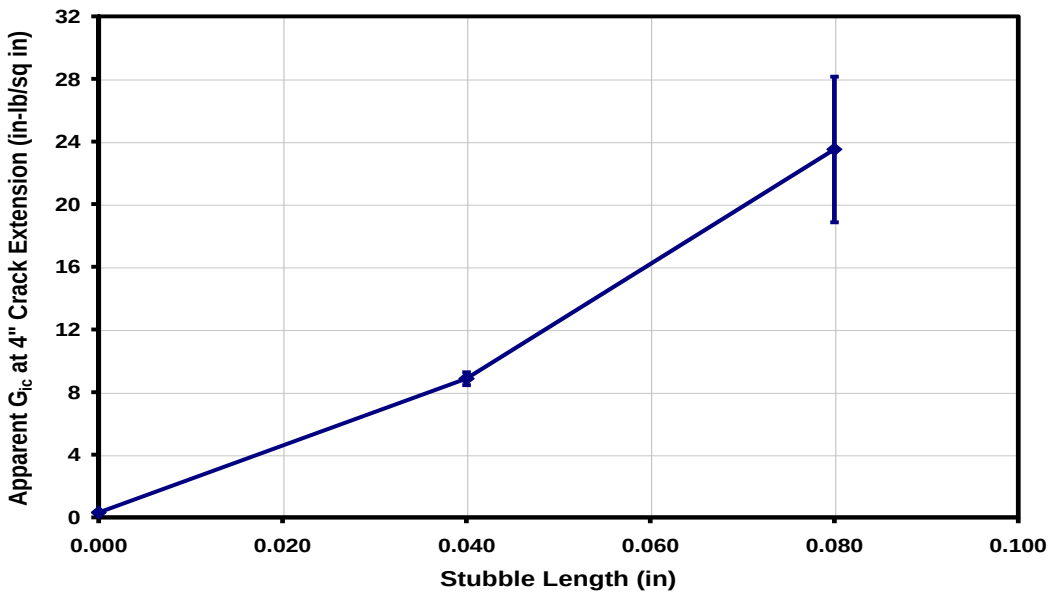

Figure 29: Effect of Stubble Length on the Apparent Gic at 4 inch Crack Extension for Co-Bonded 18 Ply Unidirectional AS4/3501-6 Graphite Epoxy with No Adhesive Layer

A general delamination toughness can be described by calculating the enclosed area under the load – displacement curve (Figure 25). This calculation was performed on the data corresponding to crack lengths between two and four inches. The average apparent G_{ic} appears to increase linearly with respect to z-pin stubble length as shown in Figure 30. It is apparent that the z-pin stubble significantly increased the overall toughness of the joint. The average unreinforced area was calculated to be only 0.33 in-lb/sq in, while the 0.040 inch long stubble had an average area of 7.7 in-lb/sq in, and the 0.080 inch long stubble had an average area of 15.5 in-lb/sq in. This corresponds to increases of about 23X to 47X. These results indicate that stubble length plays a significant role in defining the joint toughness, at least up to lengths of 0.080 inch.

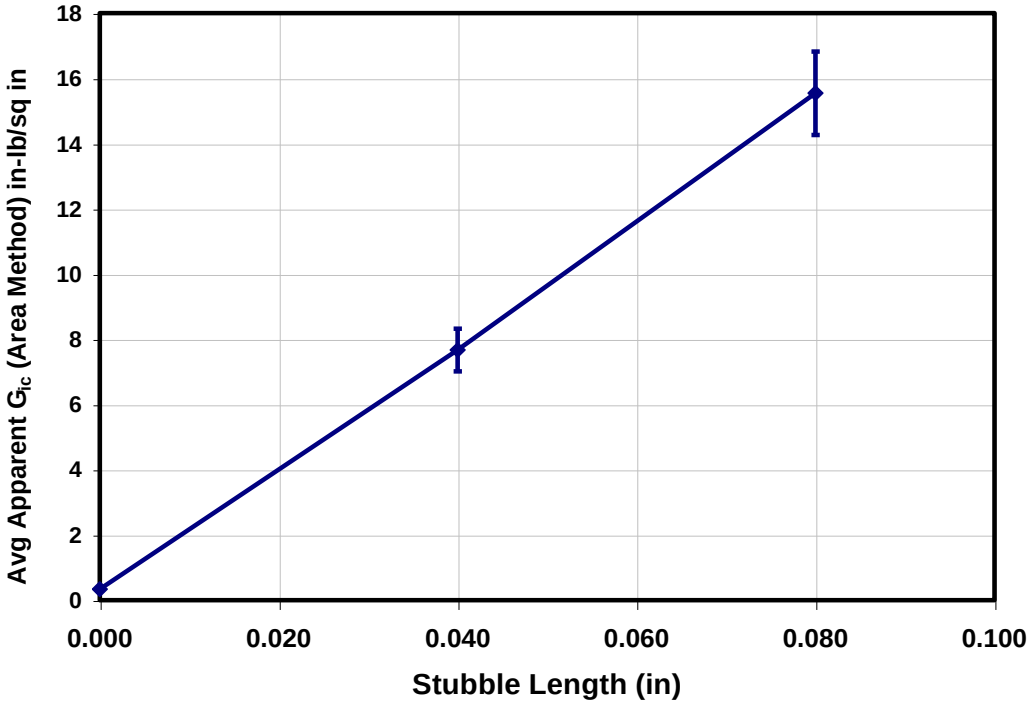

Figure 30: Effect of Stubble Length on the Average Apparent Gic Using the Area Method for Co-Bonded 18 Ply Unidirectional AS4/3501-6 Graphite Epoxy with No Adhesive Layer

4.2.2 0.040" to 0.080" Stubble, 0.011" to 0.020" Diameter Pins, 2% to 4% Aerial Density

The previous results clearly showed a significant improvement in Mode I toughness with increased stubble length from 0.040 to 0.080 inches[xiii]. Unfortunately, it only considered 0.020 inch diameter z-pins with an aerial density of 2%. The results in this section increase the correlation range to include 0.011 inch diameter pins and 4% aerial density. The original objective was to test multiple replicates of each combination. The stubble was fabricated using a stack of alternating layers of polyester peel ply and non-porous Teflon as stated above and shown in Figure 8 and Figure 9. Upon removal of the peel plies, many of the pins pulled out of the composite and remained in the peel ply. Fortunately there was a large enough region with acceptable stubble that DCB specimens could be fabricated. As a result of the missing pins, fewer replicates could be tested than originally planned, and the ones that were tested contained a slightly smaller density of pins than indicated on the test matrix.

Figure 31 and Figure 32 graphically show the effect of stubble length and density on the Mode I load carrying capability and the energy release rates of stubble reinforced composite joints. The nomenclature on the legend includes the pin diameter, stubble height, and aerial density. The 0.011 inch diameter stubble specimens lost more pins during fabrication than the 0.020 inch diameter stubble, so the results for the smaller diameter stubble are lower than expected but still show a significant improvement over the unreinforced specimens. It is apparent that the

maximum load and the maximum G_{ic} significantly increased with increasing density and stubble height.

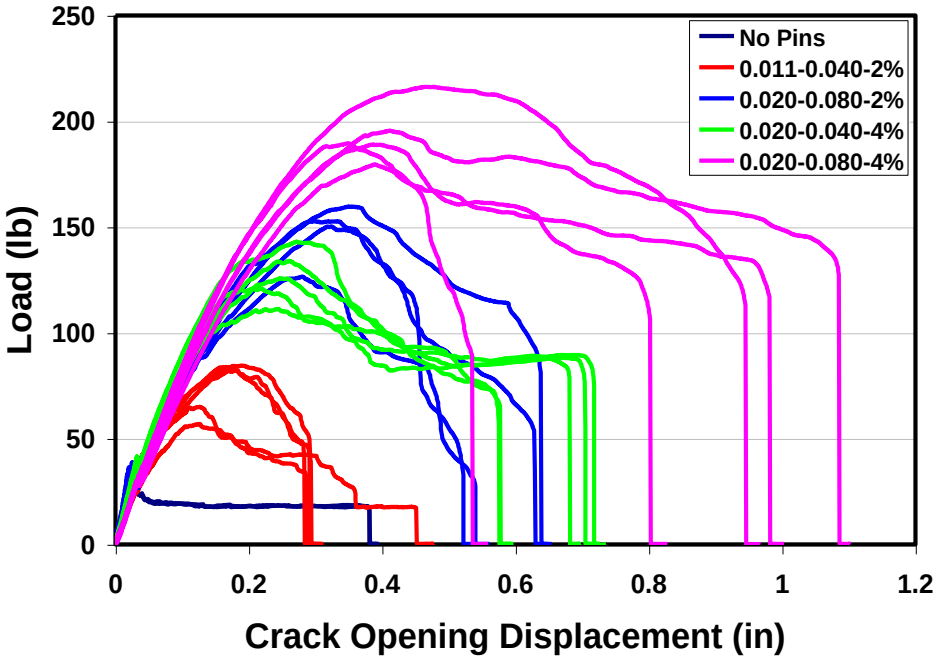

Figure 31: Effect of Z-Pin Stubble on the Mode I Load–Extension Behavior of Co-Bonded Unidirectional AS4/3501-6 Graphite Epoxy

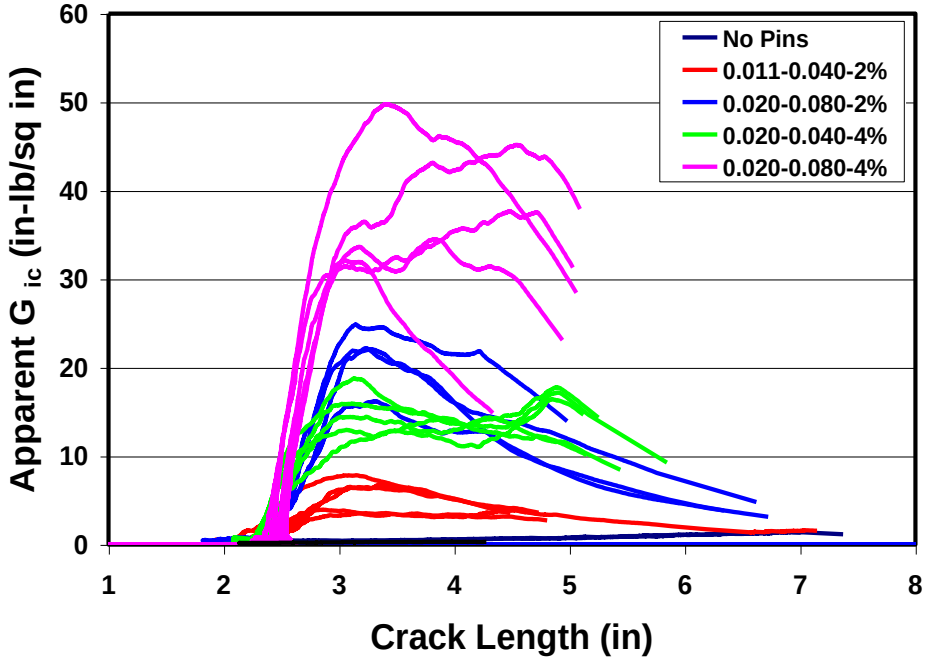

Figure 32: Effect of Z-Pin Stubble on the Mode I Energy Release Rate for Co-Bonded Unidirectional AS4/3501-6 Graphite Epoxy

Figure 33 and Figure 34 summarize the results for apparent critical energy release rate for initiation and average apparent energy release rate calculated using the area method, respectively. The error bars show one standard deviation. The column labels include the pin diameter, stubble height, and aerial density. It is clear from Figure 33 that the stubble reinforcement did not increase the energy required for crack initiation. This result is in agreement with previous studies [xiii]. The pins do not carry a significant amount of load across the interface until a crack has already initiated. Figure 34 clearly shows the benefit of the pins for delamination resistance. The average apparent energy release rate is generally a measure of joint toughness. A higher value indicates a higher resistance to crack propagation. The unreinforced joints had an average critical energy release rate for propagation of 0.6 in-lb/sq in, while the intermediate stubble reinforced joints had average values of 10 to 12 in-lb/sq in and the longer, denser stubble specimens had average values of 28 in-lb/sq in. The results summarized in Figure 35 clearly show that all of the stubble reinforced specimens performed much better than the specimens with no pins. It also shows the clear advantage of using 4% aerial density with longer stubble height.

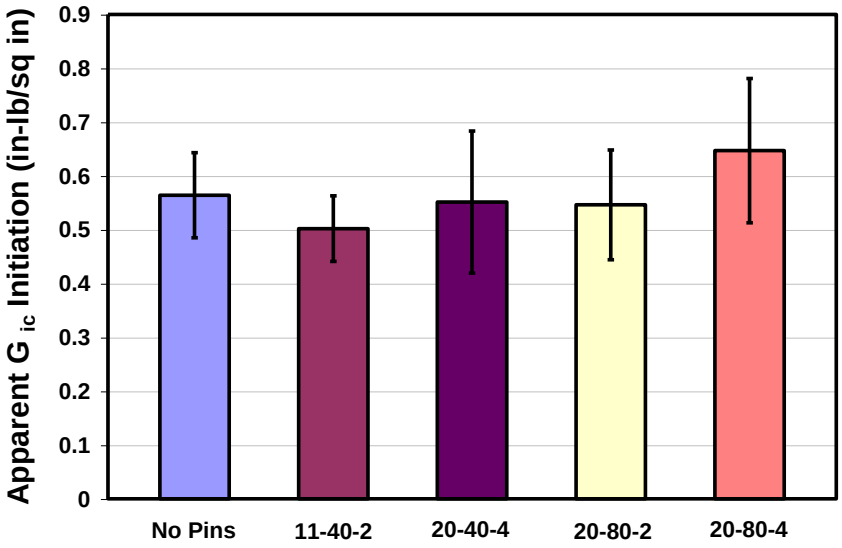

Figure 33: Effect of Z-Pin Stubble on the Mode I Critical Energy Release Rate for Initiation

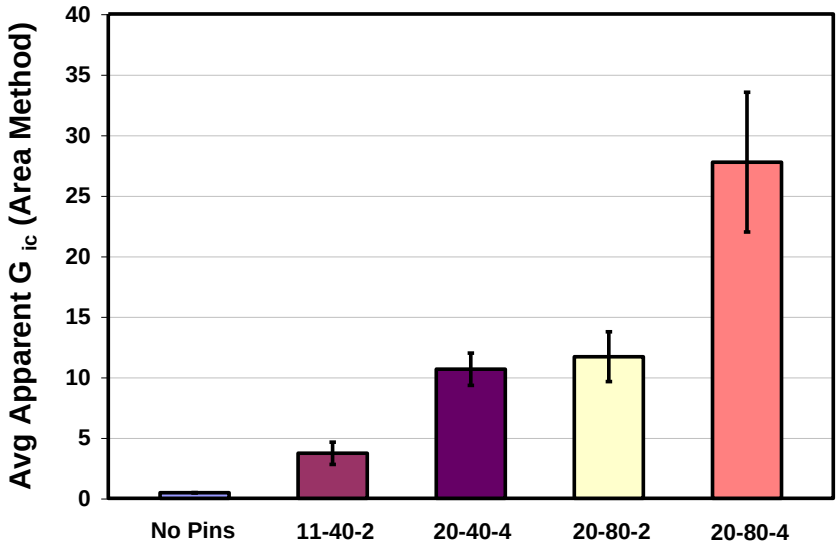

Figure 34: Effect of Z-Pin Stubble on the Average Mode I Critical Energy Release Rate Calculated Using the Area Method

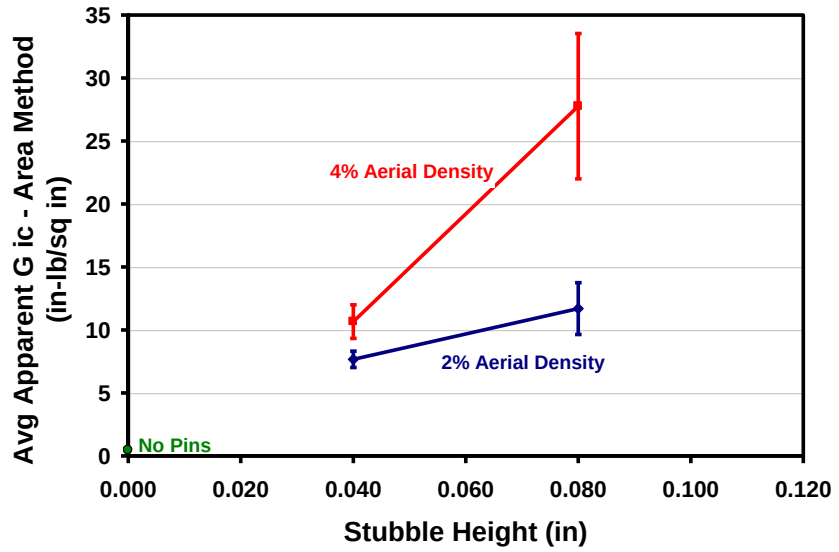

Figure 35: Effect of Z-Pin Stubble Height and Density on the Average Mode I Critical Energy Release Rate Calculated Using the Area Method

4.2.3 0.125" to 0.250" Stubble, 0.020" Diameter Pins, 2% to 4% Aerial Density

The ultimate goal of the current research project is to determine the effect of "full-depth" co-bonded z-pin stubble reinforced composites on the Mode I properties. Double cantilever beam tests were performed on 0.125 and 0.250 inch long stubble specimens. Manufacturing and testing trials were performed on specimens that were fabricated both with and without the second ultrasonic step. The specimens without the second ultrasonic step relied totally on the autoclave heat and pressure to seat the second composite on the z-pin stubble. Figure 36 shows a

photograph of a typical 0.250 inch long stubble specimen without the second ultrasonic step. The gap at the joint indicates that the specimen did not achieve 100% compaction during the cure.

Figure 36: Photograph of 0.125 inch Stubble Specimen without 2nd Ultrasonic Step

Figure 37 compares the Mode I loading characteristics of co-cured z-pinned composites to 0.125 inch long stubble reinforced composites. The specimens with the new second ultrasonic step (red-dashed line) and without the new second ultrasonic step (green-dotted line) are shown. For the 2% aerial density shown in Figure 37a, it can be seen that the overall maximum load achieved for the three variants all fall in approximately the same range of 300 to 380 lb, but the co-cured specimens generally reached a slightly higher load. Another observation is that after the first major load drop, the co-cured specimens experienced four to five repeated load cycles on the order of 50 to 100 lb, while the stubble reinforced specimens experienced a single larger load drop of 150 to 200 lb. This behavior indicates that the co-cured specimens tended to fail one row of pins at a time, but the stubble specimens failed multiple rows simultaneously.

For the 4% aerial density shown in Figure 37b, it can be seen that the overall maximum load achieved for both the co-cured and the stubble reinforced specimens with the second ultrasonic step fall in approximately the same range of 300 to 400 lb, but the stubble specimens without the second ultrasonic step only achieved on the order of 250 lb. Also, after the first major load drop, the stubble specimens with the second ultrasonic step experienced four to five repeated load cycles on the order of 50 to 100 lb, while the co-cured specimens experienced a single larger load drop of 150 to 200 lb. Finally, it should also be noted that the stubble specimens without the second ultrasonic step did not experience the usual zig-zag loading characteristics since they did not fail at the mid-plane. The failure initiated at the gap due to non-compaction and continued to grow interlaminarly above the z-pins.

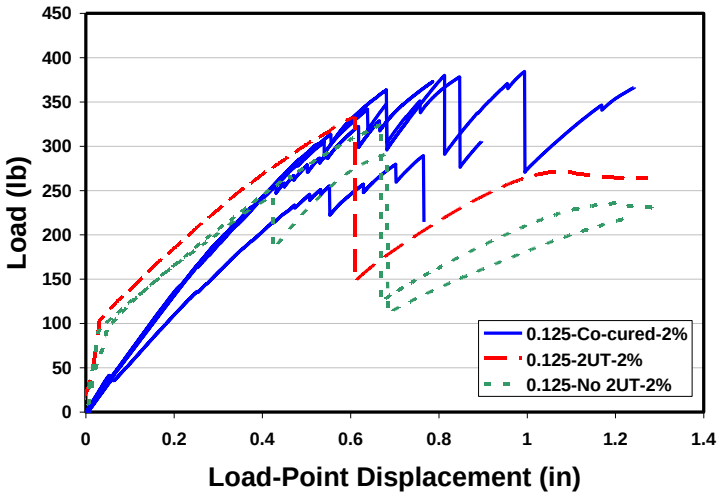

(a)

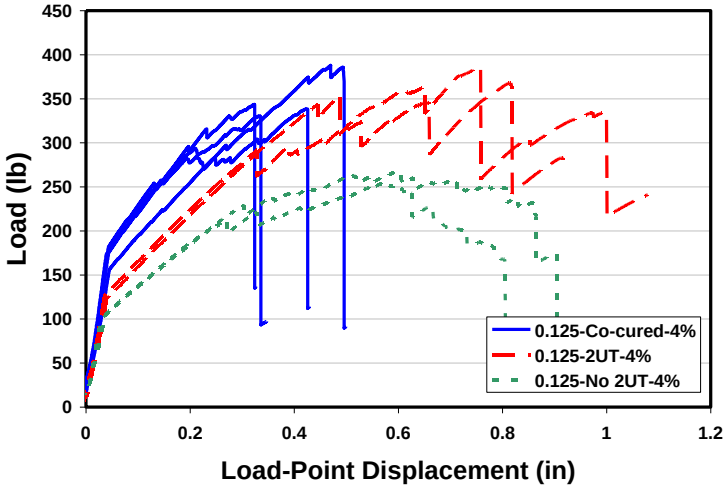

(b)

Figure 37: Effect of Manufacturing Process on the Mode I Load-Carrying Capability of 0.125 inch Stubble Reinforced Composite DCB specimens - (a) 2% (b) 4%

Figure 38 displays the equivalent data as Figure 37 but for 0.250 inch long stubble instead of 0.125 inch long stubble. The 2% aerial density results shown in Figure 38a qualitatively indicate that the stubble reinforced composites with the second ultrasonic step achieved the highest loads (400 – 450 lb) during Mode I loading. The co-cured z-pinned composites and half of the stubble reinforced composites without the second ultrasonic step failed at approximately 300 to 350 lb, while the other half of the stubble specimens without the second ultrasonic step failed at very low loads. These failures can be attributed to the large gap in the joint shown in Figure 36.

For the 4% aerial density shown in Figure 38b, it should first be noted that only one specimen for each stubble variant is shown due to the fabrication issue with the neoprene mentioned previously and shown in Figure 19. It can be seen that the co-cured z-pinned specimens achieved the highest maximum loads on the order of 350 to 600 lb, but that there is relatively high scatter in the data.

The stubble specimen with the second ultrasonic step achieved the second highest load of approximately 400 lb, while the specimen without the second step reached only 300 lb.

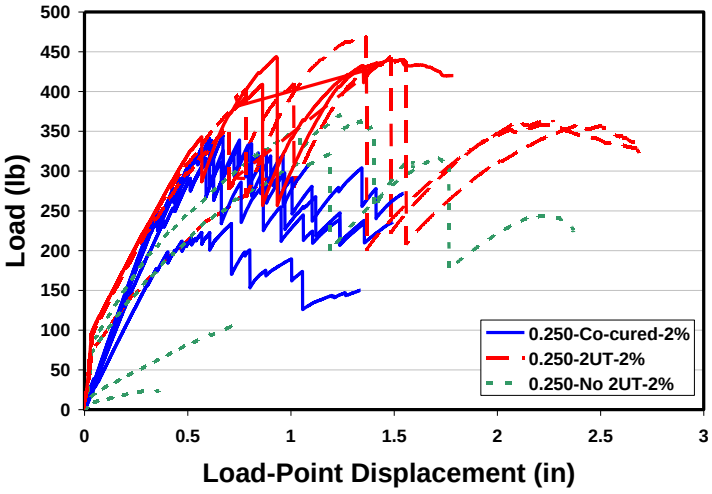

(a)

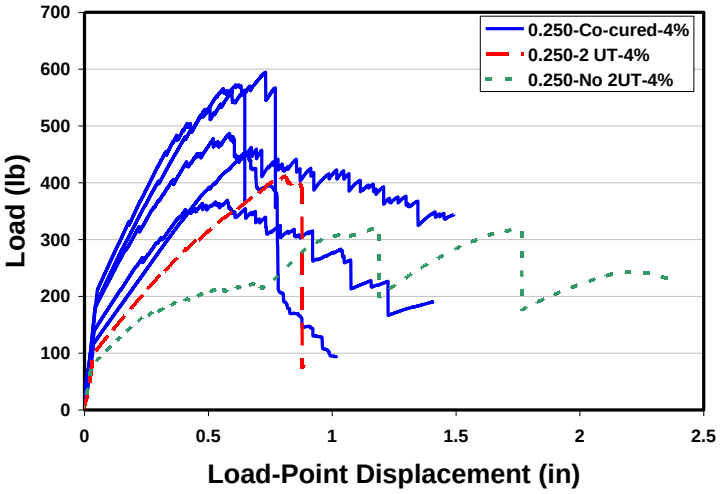

(b)

Figure 38: Effect of Manufacturing Process on the Mode I Load-Carrying Capability of 0.250 inch Stubble Reinforced Composite DCB specimens - (a) 2% (b) 4%

Another piece of data that was collected for each test was the initial load drop. The initial load drop was defined as the point at which the load first decreased a minimum of ten pounds. Figure 39 displays the results for the (a) 2% and (b) 4% aerial density as a function of stubble height. The error bars show one standard deviation. For the 2% aerial density, Figure 39a shows that the stubble specimens with the second step achieved the highest loads before the initial failure while the other two variants experienced initial failure at lower loads. Of even more interest are the 4% aerial density results. Figure 39b indicates that the co-cured and stubble specimens with the second step experienced initial failure at approximately the same loads (250 to 350 lb), but the specimens without the second step experienced the first load drop 100 to 200 lb sooner. This is another result of the poor consolidation achieved by autoclave heat and pressure during cure.

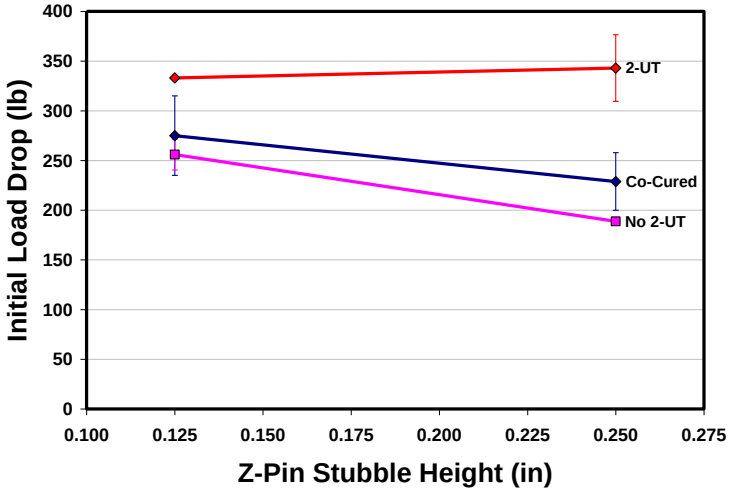

(a)

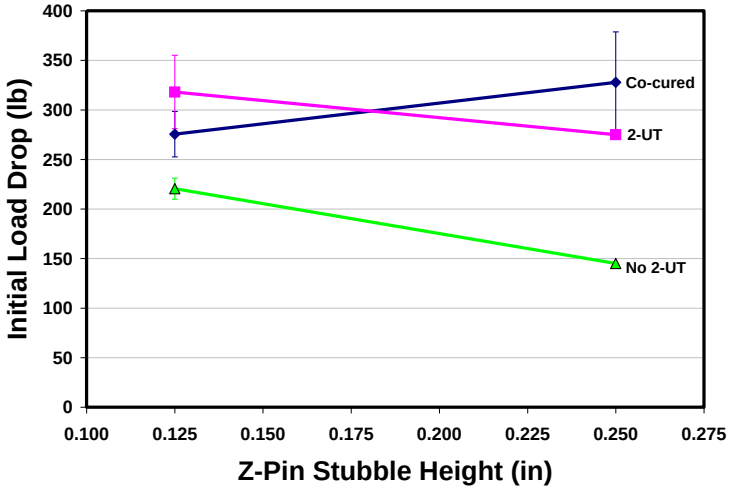

(b)

Figure 39: Effect of 2nd Ultrasonic Step on Initial Mode I Load Drop at (a) 2% and (b) 4% Aerial Density

Figure 40 compares the maximum Mode I loading results of the current study with the results of the previous efforts during which shorter stubble lengths were characterized. The data shown in Figure 40 only include the specimens that were fabricated using the second ultrasonic step. The error bars show one standard deviation of the data.

The first observation is that the baseline specimen with no z-pins achieved a maximum load of only about 35 lb. It is obvious that the z-pin stubble in the joint significantly improves the Mode I load carrying capability of composites. Next, the effect of aerial density was minimal. Increasing the aerial density from 2% (dark blue) to 4% (magenta) only increased the maximum load carrying

capability by approximately 50 lb. On the contrary, increasing the stubble length significantly increased the Mode I properties. Going from a stubble height of 0.040 inches to a stubble height of 0.125 inches increased the maximum load by approximately 300 lb. The conclusion is that significant benefits in crack resistance will be realized up to z-pin embedded depths of 0.125 inches. Finally, a knee in the curve was discovered around 0.125 inches. Doubling the stubble height from 0.125 inches to 0.250 inches only increased the maximum load by 50 to 100 lb. Considering the difficulty in fabricating the 0.250 inch stubble, the small increase in load carrying capability is probably not worth the extra effort.

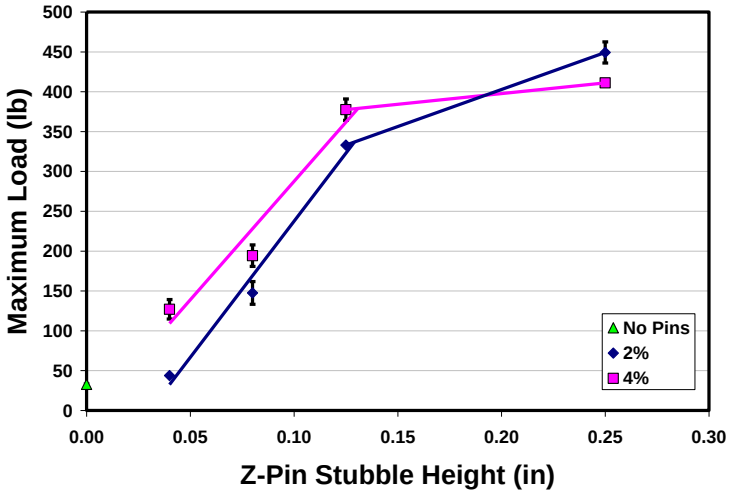

Figure 40: Effect of Stubble Height and Aerial Density on the Maximum Mode I Load-Carrying Capability

Finally, the critical energy release rates were determined for the stubble reinforced composites. A modified beam theory [x] was used to analyze the fracture properties, while an average energy release rate value was determined based on the area method. Figure 41 shows the results of the entire effort, including unreinforced composites through stubble lengths of 0.250 inches. The average energy release rate provides a toughness metric for the joint that generally describes its resistance to crack growth over an extended distance (1 to 3 inches). First, it is apparent that the baseline specimens with no z-pins have extremely low values for average G. The failure of the baseline specimen was catastrophic, so once the crack started to grow there was very little resistance to continued growth and very little enclosed area under the load displacement curve. Next, similar to the maximum load data, the value added by increasing the aerial density from 2% to 4% is only about 10 in-lb/sq in, but increasing the stubble height significantly improves the joint toughness. For the 2% specimens, increasing the stubble height from 0.040 inches to 0.250 inches increased the average G from 10 to 90 in-lb/sq in. A similar trend was seen in the 4% specimens up to a stubble height of 0.125 inches, but increasing the stubble height of the 4% specimens to 0.250 inches created a situation of failure above the pins resulting in low toughness.

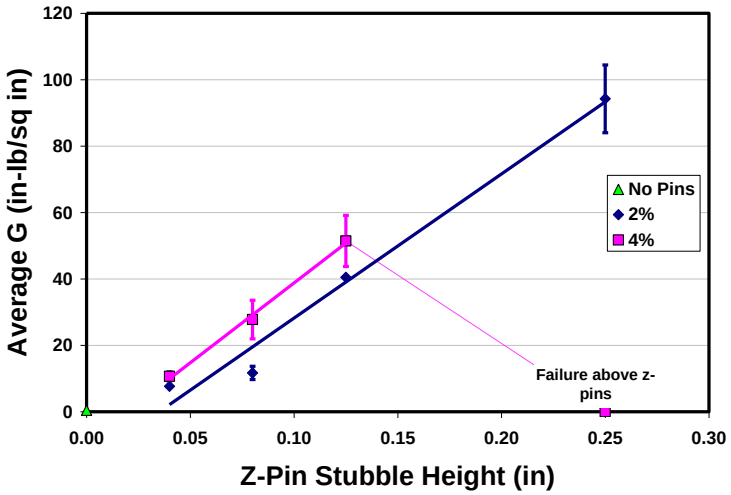

Figure 41: Effect of Stubble Height and Aerial Density on the Average Apparent Mode I Energy Release Rate (Area Method)

5 CONCLUSIONS AND RECOMMENDATIONS

5.1 Peel Ply Screening

A new approach to make through-thickness z-pinned joints compatible with the co-bonding process was described and shown to be successful. Previous attempts to use z-pin stubble in a co-bonding operation were limited to approximately 0.030 inch z-pin depths. The new two-step approach was shown to produce pristine specimens with stubble lengths up to 0.250 inch.

A peel ply screening study was conducted since peel plies began as an essential part of the new fabrication process. Nylon, fiberglass, Kevlar, and polyester peel plies all left the composite surface with relatively the same roughness, in the range of 100 to 400 micro-inches. Polyester and nylon peel plies were found to be the easiest to remove from a z-pin stubble field. The polyester peel plies came off the surface very cleanly without leaving any fibers on the stubble, while the other materials left a few to a large number of fibers.

Next, an experimental study was conducted to determine the effect of peel ply material and grit blasting on the Mode I delamination toughness of z-pin stubble reinforced composite joints. Co-bonded DCB specimens were made from 24 ply quasi-isotropic AS4/3501-6 graphite epoxy with one layer of AF191 film adhesive in the interface. The study showed that the largest effect was the result of including film adhesive in the joint. The G_{ic} for initiation and the maximum Mode I load all fell within the same experimental scatter for each peel ply material, each surface preparation condition, and for both unreinforced and 0.030 inch long stubble reinforced DCB specimens. Although no correlation was found up to the maximum load, the joint behavior after the crack began to propagate was strongly influenced by the presence of z-pin stubble. The 0.030 inch long stubble was found to significantly increase the joint "toughness" as defined by the area under the load-displacement plot; but no correlation was found between the "toughness" and the peel ply material or grit blasting. It is suggested that the peel ply material be selected wholly based on ease of removal and cleanliness of bonding surface. For this reason, a polyester peel ply was used for most of this project until the rubber sheet material became the preferred approach.

5.2 Effect of Stubble Length on Mode I Properties (0.040" to 0.080")

Next, an experimental study was conducted to determine the effect of stubble length on the Mode I delamination resistance of co-bonded 18-ply unidirectional AS4/3501-6 graphite epoxy with no adhesive. This study was made possible by the novel two-step ultrasonic approach for reinforcing co-bonded composite joints using z-pin stubble. DCB specimens were made with z-pin stubble lengths up to 0.080 inches. It was found that the maximum Mode I load, apparent Gic at four inch crack extension, and joint "toughness" all increased relatively linearly as the stubble length was increased from 0.040 to 0.080 inch. It is concluded that the Mode I failure load of a z-pinned joint is governed by the frictional loading between the pin and the epoxy matrix. As the z-pin length increases, the number of active rows of pins in a crack front increases, enabling the joint to carry more load during crack propagation.

The 0.040 and 0.080 inch stubble reinforced joints were characterized using DCB testing. It was found that the presence of stubble did not improve the critical energy release rate for crack initiation but it did significantly improve the overall joint toughness as measured by the average strain energy release rate. Increasing both the stubble height and the aerial density increased the

resistance to crack growth. The authors' recommendation is to use z-pin reinforcement in composite joints when resistance to crack propagation is critical for the component. One example would be a composite aircraft wing containing fuel tanks. A ballistic impact to the fuel bay would produce very large out of plane loads on the joints, which z-pins would help resist. If co-curing is the best choice for fabrication then traditional through thickness z-pin reinforcement should be used. If co-bonding is the preferred assembly approach, the use of z-pin stubble is the only option for reinforcement. The results of this study indicate that significant improvements can be achieved through longer, denser z-pin fields. Also, the smaller diameter pins (0.011 inch) were more difficult to work with during this study since many pins pulled out of the composite during fabrication and the uncured composite was more difficult to seat on the stubble without crushing or buckling the pins.

5.3 Rubber Material Screening

The ultimate goal of this research study was to develop a repeatable fabrication process for long, dense z-pin stubble reinforced composite joints and to determine the effect of the stubble on the Mode I properties. While making the first two sets of stubble panels, several z-pins pulled out of the composite during removal of the polyester peel plies. The conclusion is that woven cloth materials should not be used in this process. A rubber sheet material screening revealed that unreinforced rubber sheet materials can be used to make stubble at least up to 0.125 inches high. Four rubber materials, including silicone, neoprene, Buna-N, and EPDM, were found to perform well for stubble fabrication.

The ultimate goal of this research study was to determine the effect of long, dense z-pin stubble on the Mode I properties. The fabrication of the specimens using the new approach with commercial strength neoprene was completely successful for the 0.125 inch long stubble, but only partially successful for the 0.250 inch stubble. One recommendation would be to use two separate layers of 0.125 inch thick neoprene instead of one layer of 0.250 inch thick neoprene. This would likely result in the complete removal of the rubber without leaving any residue.

5.4 Effect of Stubble Length on Mode I Properties (0.125 to 0.250 inch)

The results of the DCB test for the longer, denser stubble indicate a variety of things. First, the second ultrasonic step in the fabrication process is very important, especially for the longer, denser stubble fields. Without it, the specimens do not achieve good compaction and fail at lower loads. The 0.125 inch long stubble with 2% aerial density z-pins might be satisfactory without the second step, but any configuration longer or denser should definitely use the second step.

Second, it was shown that z-pin stubble significantly increases the maximum Mode I load carrying capability. The stubble height played a more important role in improving the performance than the aerial density. Also, a knee in the curve was found at 0.125 inch long stubble, indicating a decreased significance in going from 0.125 inches to 0.250 inches.

Finally, the toughness of the joint as defined by the area method was significantly improved with the addition of z-pin stubble. Similar to the maximum load, increasing the aerial density did not improve the toughness as much as increasing the stubble height. It was also determined that the failure mode of the 0.250 inch stubble specimen with 4% aerial density changed from crack propagation through the mid-plane to interlaminar failure above the z-pins.

6 ACKNOWLEDGMENTS

The authors would like to acknowledge Ron Schmidt of Lockheed Martin for his technical guidance and advice. Larry Mack and Richard Wiggins of SelecTech Services are also appreciated for their support in composite fabrication and testing. Finally, Brian Smyers and Philip Knoth provided excellent support under pressure.

7 REFERENCES

[i] L. C. Dickinson, G. L. Farley, and M. K. Hinders, "Translaminar Reinforced Composites: A Review," Journal of Composites Technology and Research, v21, n1, 3-15 (1999)

[ii] D. Cartié and I. K. Partridge, "Z-pinned composite laminates: Improvements in delamination resistance," Proceedings of the 5th Intl Conf on Deformation and Fracture of Composites, London, 18-19 March 1999

[iii] I. K. Partridge and D. Cartié, "Increasing delamination resistance of composites by Z-fibre pinning," Proc ACUN-3 'Technology Convergence in Composites Applications", UNSW, Sydney, Australia, 6-9 February 2001

[iv] D. Cartié and I. K. Partridge, "Delamination behaviour of Z-pinned laminates," Proceedings of ICCM12, Paris, 5-9 July 1999

[v] D. Cartié, A. J. Brunner, and I. K. Partridge, "Effects of mesostructure of z-pinned laminates on their crack control characteristics," Proc 3rd ESIS-TCH Conference, 15-18 Sep 2002, Switzerland

[vi] A. Clarke, E. Greenhalgh, C. Meeks, and C. Jones, "Enhanced structural damage tolerance of CFRP primary structures by z-pin reinforcement," Proc. 44th AIAA/ASME/ASCE/AHS Structures, Structural Dynamics, and Materials Conference, 7-10 Apr 2003, Norfolk, VA

[vii] Aztex, Inc., www.zfiber.com

[viii] McMaster Carr on-line product catalog, http://www.mcmaster.com, cited Mar 1, 2006.

[ix] ASTM Standard D5528-94a, "Standard test method for Mode I Interlaminar Fracture Toughness of Unidirectional Fiber-Reinforced Polymer Matrix Composites," *Annual Book of ASTM Standards*, 272 (1994)

[x] K. A. Dransfield, L. K. Jain, and Y. W. Mai, "On the effects of stitching in CFRPs – I. Mode I delamination toughness," Composites Science and Technology 58 (1998) 815-827

[xi] J. R. Reeder, "An evaluation of mixed mode delamination failure criteria", NASA Technical Memorandum 104210, http://techreports.larc.nasa.gov/ltrs/PDF/NASA-92-tm104210.pdf

[xii] H-Y. Liu, W. Yan, S-C. Dai, and Y-W. Mai, "Experimental study on z-pin bridging law by pull-out tests," Proc. 44th AIAA/ASME/ASCE/AHS Structures, Structural Dynamics, and Materials Conference, 7-10 Apr 2003, Norfolk, VA

[xiii] S. Clay, A. Pommer and R. Jones, "Novel Two-Step Ultrasonic Approach for Reinforcing Co-bonded Composite Joints Using Z-FiberTM Stubble," Proceedings of the AIAA Structures, Structural Dynamics, and Materials Conference, 2005.

NOMENCLATURE

ASTM	=	American Society for Testing and Materials
AW	=	aerial weight
DCB	=	double cantilever beam
E_{11}^{F}	=	flexural modulus
E_{33}	=	transverse modulus
EPDM	=	ethylene-propylene-diene-monomer
FDA	=	Food and Drug Administration
G_{13}	=	transverse shear modulus
G_{ic}	=	Critical Mode I energy release rate
in-lb/sq in	=	inch pounds per square inch
lb	=	pounds
in	=	inches
pcf	=	pounds per cubic foot
psi	=	pounds per square inch
UT	=	ultrasonic